Ground Winds Experienced by the Space Launch System Rocket on the Pad before the Artemis I Launch

Jeremy T. Pinier*
NASA Langley Research Center, Hampton, VA 23681, USA

Over the course of development of the Space Launch System (SLS) human-rated heavy-lift launch vehicle, the magnitude and nature of the ground winds experienced by the rocket and its Mobile Launcher (ML) on Pad 39B at the NASA Kennedy Space Center (KSC), became a more critical environment that required characterization as well as a more accurate prediction of the vehicle and ML response in the form of detailed wind loads. The numerous reasons for the sensitivity of the launch system to these ground winds and the growing importance of high fidelity rollout and launch pad wind loading estimates are discussed in this article. A description of the wind measurement instrumentation at and around the Launch Complex is provided. A methodology is developed to estimate from these raw anemometer measurements the winds experienced by the rocket and mobile launcher on the launch pad, either in real time or during post-processing. An analysis is then performed and documented on the 121 days worth of wind measurements recorded while the SLS vehicle was secured on the pad during various launch attempts and wet dress rehearsals. This included the occurrence of a tropical storm that evolved into a named hurricane by the time it arrived on Cape Canaveral and hit the vehicle while sitting on the launch pad. Plans for further developments to improve on this predictive capability in preparation for the Artemis II mission are also presented.

Nomenclature

ATT	=	Aerodynamics Task Team
CFD	=	Computational Fluid Dynamics
CT	=	Crawler-Transporter
$DSNE$	=	Design Specification for Natural Environments
FRR	=	Flight Readiness Review
$F\&M$	=	Aerodynamic Forces and Moments
KSC	=	Kennedy Space Center
$LaRC$	=	NASA Langley Research Center
LCC	=	Launch Commit Criteria
LPS	=	Lightning Protection System
LT	=	Lightning Tower
ML	=	Mobile Launcher
MLP	=	Mobile Launch Platform
MLT	=	Mobile Launch Tower
MMT	=	Mission Management Team
$MSFC$	=	Marshall Space Flight Center
$NASA$	=	National Aeronautics and Space Administration
SLS	=	Space Launch System
TLI	=	Trans-Lunar Injection
VAB	=	Vehicle Assembly Building
WDR	=	Wet Dress Rehearsal

*SLS Aerodynamics Task Team Member, Configuration Aerodynamics Branch, D301, Associate Fellow AIAA

Symbols

Az = Wind azimuth (i.e., direction from which the wind is coming)
V = Wind velocity magnitude
u = Westerly component of the wind velocity vector (i.e., positive West to East)
v = Southerly component of the wind velocity vector (i.e., positive South to North)

I. Introduction

The Space Launch System (SLS) is a family of evolvable super heavy-lift launch vehicles that will be NASA's workhorse for the next decades carrying both humans and heavy payloads into deep space, specifically cislunar space in a first phase for NASA's Artemis Program. The nation is returning humans to the Moon with a long-term sustainable goal of learning how to live on another planet, including producing our own energy, consumable resources (water, oxygen, hydrogen), deploying habitats, and manufacturing or assembling structures and surface infrastructure for a long term presence to achieve ambitious scientific goals near the lunar South pole, where water ice resides inside craters that have never seen the light of day. The first test flight of the SLS occurred on November 16th, 2022 at 01:47:44am Eastern Standard Time with the launch of an uncrewed SLS Block 1 vehicle that took an Orion crew capsule on a journey to the Moon and back, validating all ground systems, launch vehicle systems, and crew capsule systems for the second flight that will this time carry a crew of four astronauts on a free-return flight to the Moon. This SLS Block 1 vehicle will be flown two more times for the Artemis II and III missions and then be replaced by the SLS Block 1B vehicle that will be the new most capable human-rated deep space super heavy-lift launch vehicle that will be able to carry humans and large payloads into a Trans-Lunar Injection (TLI) trajectory, with a total TLI capability of 38 metric tons. Figure 1 shows the outer mold line and Payload-to-TLI capability of this evolvable family of human-rated launch vehicles. All detailed specifications of the SLS Block 1 vehicle are found in the SLS Reference Guide [1].

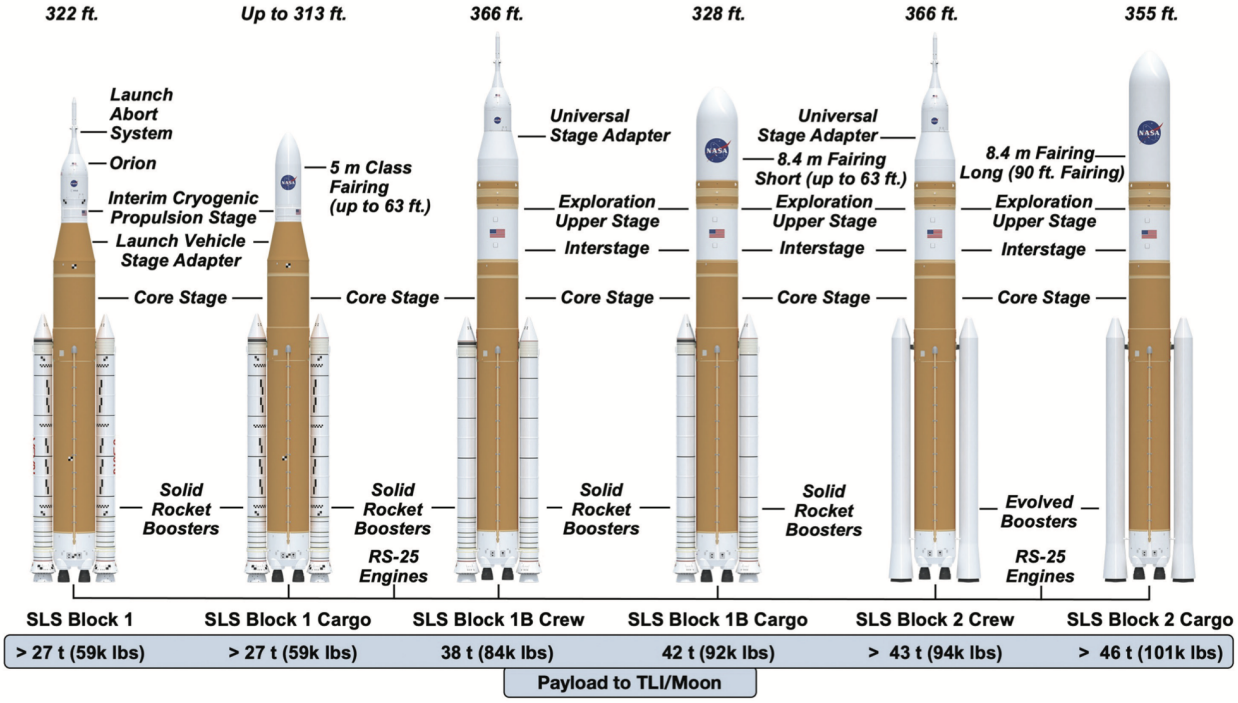

Fig. 1 Illustration of the Space Launch System family of vehicles with description of major elements and payload capabilities. Payload units are metric tons (t).

In order to characterize the environments that the SLS vehicle flies through as it moves within our atmosphere, a number of complex aerodynamic databases are developed using both wind tunnel testing and Computational Fluid Dynamic (CFD) simulations, from very low speed flows at and before liftoff to high-supersonic flows as the boosters separate and the core stage leaves Earth's atmosphere, as reported in overview papers by Blevins et al. [2] and Pinier et al. [3]. One of these environments is the prelaunch and liftoff ground winds environment, which has been developed, analyzed and described in detail by Pinier et al. [4], Chan et al. [5], Collins et al. [6], Mears et al. [7], Wignall et al. [8], and Walker et al. [9]. Those environments were always developed in very controlled test facilities and simulations with precise boundary conditions, or very well known and controlled inputs for the most accurate possible aerodynamic outputs. This type of work is fundamental in defining design environments for building a robust and reliable launch vehicle. The Artemis I flight and the time leading up to launch provided a unique opportunity to collect large amounts of full-scale, real-life data, albeit more noisy and uncertain outputs with sparse inputs. Accuracy (or lack thereof) in the inputs and outputs is traded for fidelity of the full-scale vehicle in real ground winds environments. This paper delves into the acquiring and post-processing of these real-world environments that will ultimately provide a way to connect ground measurements to reality.

II. Ground Winds and the SLS, ML, and Crawler-Transporter

The final assembly of the SLS launch vehicle major stages and components is completed vertically inside the Vehicle Assembly Building (VAB) and directly on the Mobile Launcher (ML). The two solid rocket boosters are stacked and mounted first, then the core stage with its four main engines is hoisted in place and mounted to the boosters. Once ready for launch, the ML and SLS are transported from inside the VAB to launch pad complex 39B using the crawler-transporter (CT). This operation is a major step in terms of complexity, time duration, and stress on all parts of the launch system. The CT advances at less than 1 mph along the 4.2 mile crawlerway made up of Alabama river rocks to launch pad 39B. From start to finish, this operation takes on the order of 10 hours. Because of the delicate nature of the transport operations, it is only accomplished when winds are very low, and sometimes overnight when conditions are ideal. However, once the ML and vehicle are secured on the launch pad, the launch system can be exposed to significant weather and winds because it can be there for extended periods of time. Before the Artemis I flight, the SLS vehicle was on the launch pad a total of 121 days, exposing it to a number of high to extreme wind events discussed in the next section. Figure 2 shows a photograph of the SLS/ML/CT system moving toward the launch pad during its first roll out of the VAB.

During the initial years of development of the Space Launch System rocket, the aerodynamic characterization of the vehicle response to ground winds environments was limited to static wind loads on the vehicle for the purposes of liftoff (post T=0) flight simulations and liftoff loads analyses. Accurate wind loads on the ML itself only came to be requested in 2018, late into the development program. Several factors motivated a new look at ML wind loads. First, the combination of increased weight of the ML, as well as increased predictions of blast loads at liftoff from engine plumes resulted in wind loads becoming a driving factor despite being the smallest of the three major loads applied. The low fidelity and, therefore, high uncertainty in the initial ML wind load estimates motivated a new effort to replace those with higher accuracy predictions. Secondly, the crawlerway conditioning team at the NASA Kennedy Space Center (KSC) that is responsible for determining the appropriate level of conditioning load applied to the gravel to compact it before transporting the vehicle and ML to the pad, was becoming concerned that early estimates of wind loads based on basic assumptions and engineering analysis may not have been appropriate, and that, if true, then the CT could dig into the gravel and come to a stop. These two factors prompted the SLS Aerodynamics Task Team (ATT) to develop novel testing capabilities to measure ML wind loads simultaneously with vehicle loads during the wind tunnel tests cited above, and to run high-fidelity CFD simulations of a more detailed ML and launch vehicle.

There are numerous reasons why this launch system has required increased attention, detailed measurements, and advanced analysis regarding ground winds, which include:

1) It is very large and tall, with stronger winds aloft. Being a slender centerbody above the boosters section, vortex shedding has a higher chance of tuning with the vehicle natural bending modes and enter a fluid-structure resonance lock-in.
2) There are two main loads applied before liftoff (including rollout): The weight of the vehicle and Mobile

Fig. 2 First SLS Block 1 vehicle rollout to Pad 39B on March 17th, 2022, showing the SLS launch vehicle, the Mobile Launcher (ML) and the Crawler-Transporter (CT) [Source: NASA, Pinier].

Launcher, and the wind loads experienced by both systems. At liftoff, the ML experiences a third load, which is the blast load from the main engine plumes and the solid rocket booster plumes. Because both the predicted weight and blast loads increased with maturity of the systems; wind loads, though smaller than weight and blast, became a critical quantity that required higher fidelity estimates.

3) The vehicle can stay on the launch pad for many days, exposing it to potentially strong weather systems. Returning the vehicle to safety in the VAB is a complex process that can take a few days, in addition to being harmful to the hardware in terms of vibrations, fatigue, and loads.
4) The flowfield interactions between the ML and the vehicle have shown to be significant for certain wind directions in the wind tunnel [4].
5) Weather at KSC can change rapidly and exhibit strong, fast-moving systems, in particular during hurricane season. Storm systems are difficult to predict, and their paths are highly variable and uncertain. The risks due to the uncertainty in the weather can be offset by an accurate prediction of vehicle wind loads on the ground, given known wind inputs.
6) A few hardware systems, like the forward attach bolts between the boosters and the core stage, were not designed for strong wind loading situations when the vehicle is untanked (bolts in low compression, or even tension) and on the launch pad.
7) For such a complex launch vehicle, increasing launch availability is both challenging and critical. There needs to be a maximum number of opportunities to launch once all systems are ready and the mission flight readiness review (FRR) is successful. In order to increase launch availability, a high-fidelity understanding of the flow and vehicle/ML response to ground winds is required in order to make better-informed decisions for rolling out to the

pad to prepare for launch, safely remaining on the pad during high wind events to be ready for the next possible launch opportunity, or rolling back to protect all systems in case of an extreme wind event.

8) Experience from the Artemis I pad stay periods and a large amount of wind measurements has given the team an opportunity to greatly improve our understanding of the nature and physics of the real flows experienced by the rocket and mobile launcher.

In response to this late need for a thorough, high-fidelity characterization of prelaunch environments, a large effort was carried out both with enhanced ground testing and CFD to provide accurate predictions of wind loads on both the ML and vehicle for winds coming from any direction. This work was documented in Collins et al. [6] and Mears et al. [7]. The computational simulations work was presented by Krist et al. [10], Ratnayake et al. [11], and Pomeroy et al. [12].

When it comes to launch operations, an accurate predictive capability for the response of the launch system to ground winds is only half of the need. The other half is being able to accurately know what level of winds are being experienced at any given moment by the launch vehicle and ML on the pad. This is a more complex task to accomplish than initially assumed, and is the main novel contribution from the work documented in this paper. The following section describes what raw wind measurements are available near the vehicle when sitting on the launch pad.

III. Wind Measurements at Launch Complex 39B

In the vicinity of the launch pads at KSC, because of the large scale of the rocket and launch tower, the openness of the area, and the proximity to the ocean, wind magnitude and direction can vary greatly spatially and rapidly in time. During prelaunch operations, it is important to know what the ground wind conditions are exactly where the rocket and launch system are located. However, the challenge is that a wind measurement instrument placed very near that location would be majorly disrupted by the close proximity of the launch vehicle and tower. During the Space Shuttle program, Pad 39B was equipped with a main wind measurement at a height of 60 feet above grade level positioned away from the launch pad. This measurement became the real time data source for a Launch Commit Criteria (LCC) tied to wind direction and magnitude. After the Shuttle program and in preparation for the Space Launch System, a new Lightning Protection System (LPS) was installed at Pad 39B that would include three lightning towers equipped with four anemometers installed at different levels. Each ultrasonic anemometer measures both wind direction and speed at a high frame rate. This section describes where exactly these measurements are taken relative to the launch vehicle and presents how those 12 raw measurements at these separate locations are post-processed and manipulated to estimate the characteristics of the wind that is experienced by the launch vehicle itself. This calculation can be made in real time to assess on-pad winds, or during post-processing to correlate winds to load measurements on various parts of the vehicle or ground equipment.

With respect to the height of the four anemometers on each tower, Fig. 3 shows an aerial photograph of the launch pad complex taken from the North-West. The three lightning protection towers are shown with the location and names associated with the twelve anemometers. For all three towers, the height above grade of anemometers A, B, C, and D are 132 ft, 257 ft, 382 ft, and 457 ft, respectively. Therefore, measurement 3C (for example) is the wind measurement on Tower 3 at the height of 382 ft. The launch pad itself is elevated approximately 60 ft above grade, which results in the height of anemometers at level A being near the base of the vehicle, anemometers at level B being near the level of the tip of the boosters, anemometers at level C are near the top of the SLS vehicle, and lastly anemometers at level D are above the ML and vehicle.

Despite these anemometer sensors being high fidelity in nature, there are three main physical limitations due to installation within the launch complex that require data to be discarded for being unreliable:

- First, for each tower, the four anemometers are mounted at the end of booms installed off a specific side of the tower, as shown in the photo in Fig. 4. Because of structural interference between the sensors and the tower itself,

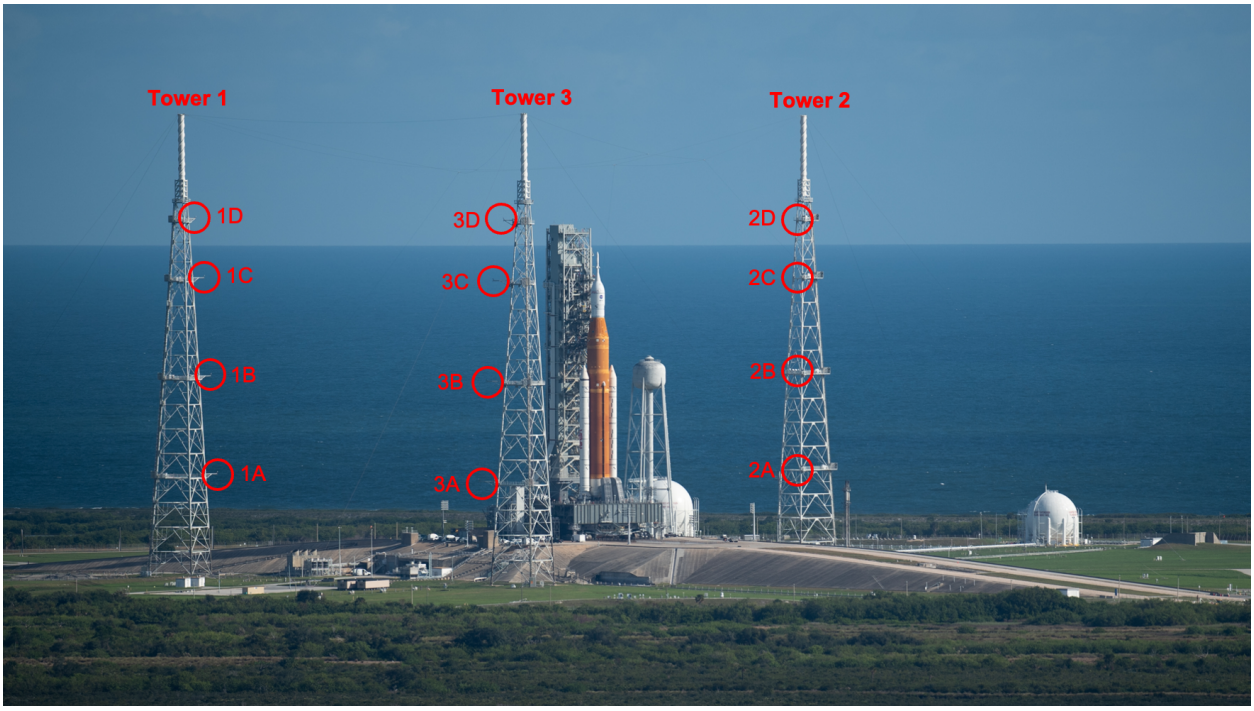

Fig. 3 Aerial photograph of Launch Complex 39B at the NASA Kennedy Space Center showing Lightning Protection System towers and locations of anemometer sensors (red circles) [Source: NASA].

Fig. 4 Photograph of an ultrasonic anemometer installed on one of the lightning towers [Source: NASA, Pinier].

conflicting angular ranges are defined for each tower where measurements may not be accurate. Figure 5 shows the three towers relative to the vehicle centerline with the conflicting angular ranges. When ground winds are coming from within those ranges, measurements are considered unreliable and should be discarded. However, because those measurements are inherently inaccurate, the data to be discarded for each tower need to be inferred from anemometer measurements on the other two towers, which would not be in their own conflicting range. An additional 10 degrees on either side of the conflicting range is discarded for the purposes of only retaining the highest quality wind data in the analysis.

- Second, it is important to note where the towers are located azimuthally in relation to the launch pad. This is because it was discovered that when the SLS and ML are located within an angular range directly upstream of a given lightning tower, the anemometer measurements for this tower were corrupted due to large wake disturbances. This

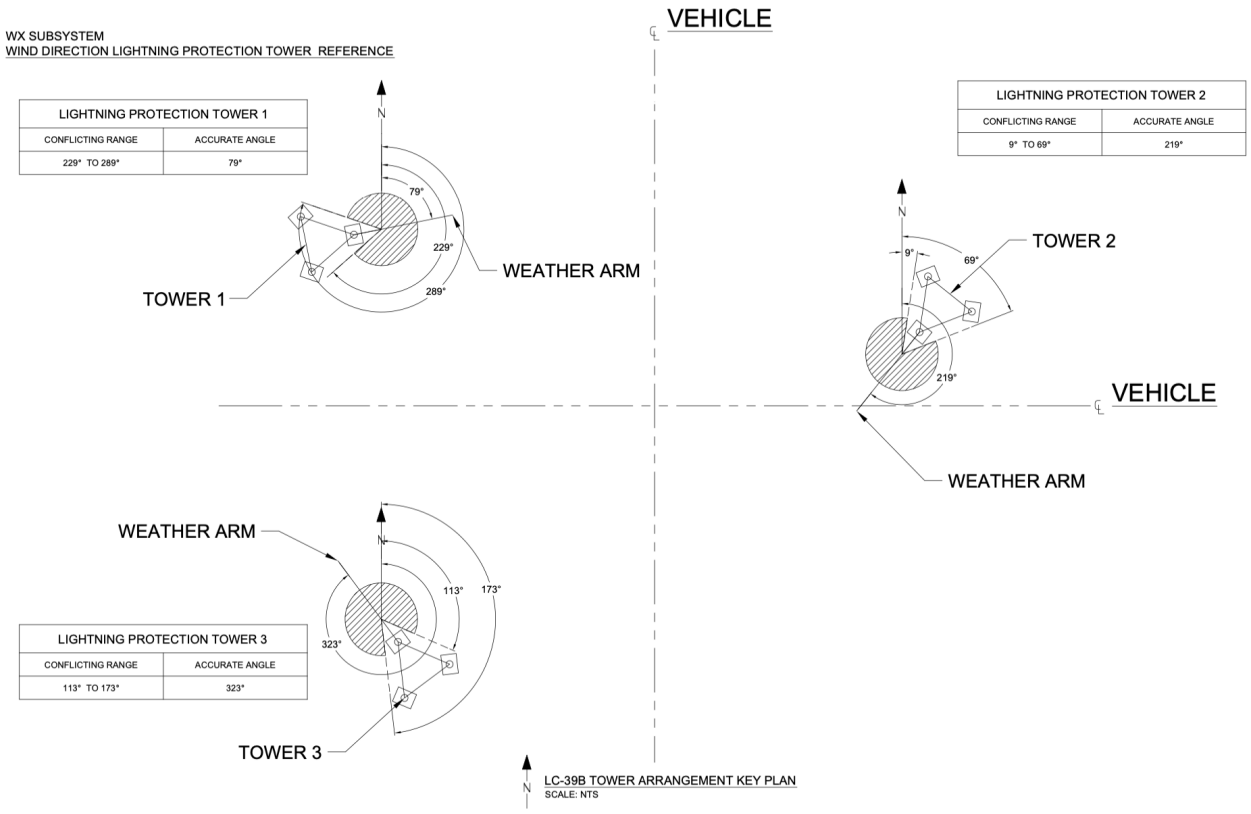

Fig. 5 Anemometer conflicting ranges from lightning tower structural interference

will be shown in the following section where raw anemometer data are documented and analyzed. This second type of anemometer data rejection range is referred to in this manuscript as the SLS/ML wake ranges. Figure 6 shows a top view of KSC launch complex 39B with the location of the three lightning protection towers in the small red circles. Lightning Tower (LT) 1 is located at a 295° azimuth from the center of the SLS core stage. LT 2 is located at a 72° azimuth from the center of the SLS core stage, and LT 3 is located at a 222° azimuth from the center of the SLS core stage. The SLS/ML wake range for each tower is defined as a range of 50 degrees centered about the heading of the SLS/ML relative to the LT, which is 180 degrees from the azimuthal position of the LT from the SLS/ML. When the SLS/ML is not on the launch pad, then this corrupted wake range does not apply. A summary of the two discarded data angular ranges for each tower is shown in Table 1.

Table 1 Discarded wind data angular ranges for anemometers on each lightning protection tower, Az is the wind direction.

Lightning Tower	Conflicting range	SLS/ML wake range
LT 1	$219° \leq Az \leq 299°$	$90° \leq Az \leq 140°$
LT 2	$359° \leq Az \leq 79°$	$227° \leq Az \leq 277°$
LT 3	$103° \leq Az \leq 183°$	$17° \leq Az \leq 67°$

- Third, a wind condition where wind direction measurements are inaccurate for all anemometers is when wind speed is close to zero. In this case, wind direction will become mathematically undefined and the data unreliable. Therefore, for all conditions where wind speed was measured to be less than 2 knots, the associated wind direction was discarded from the dataset.

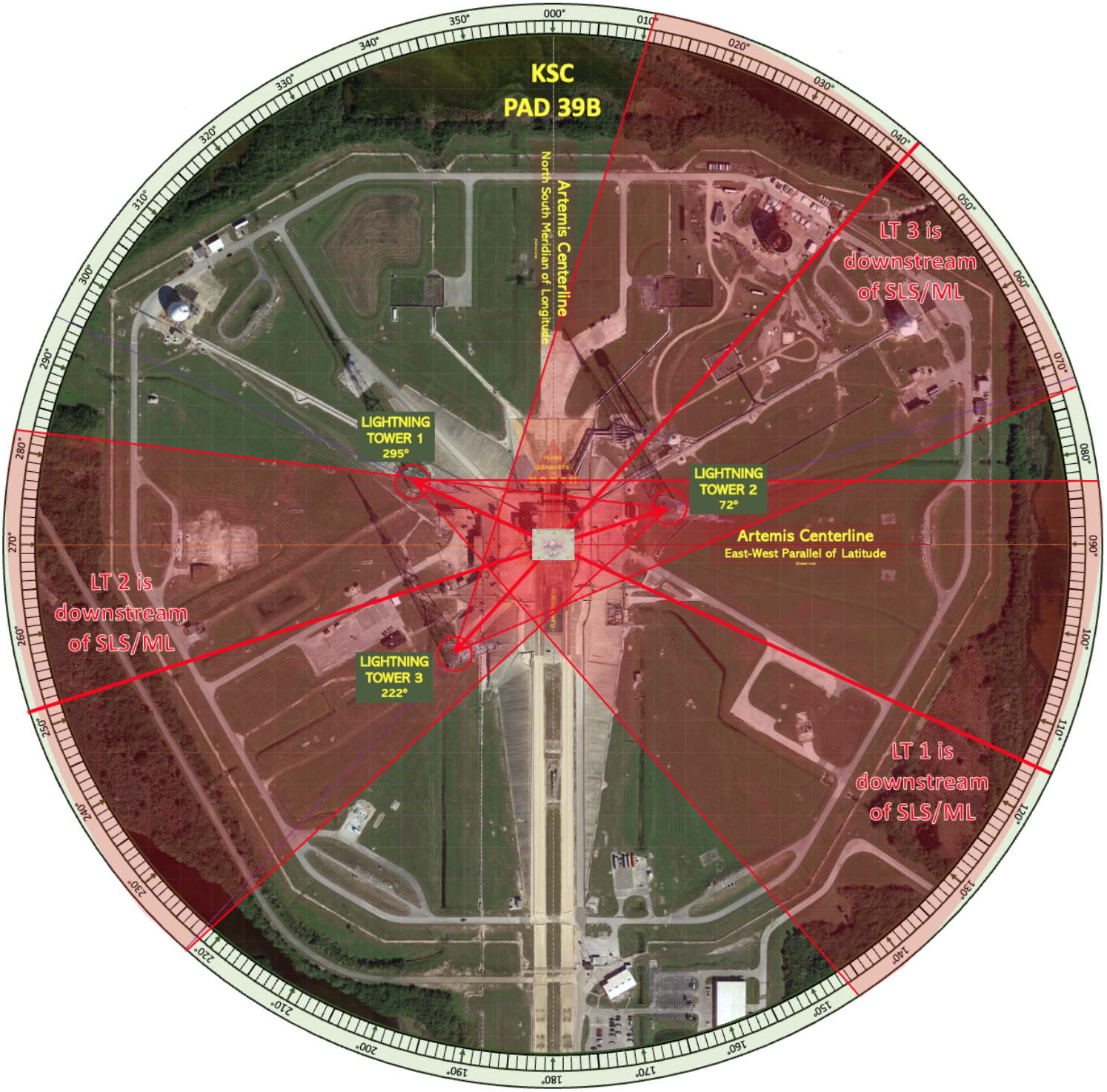

Fig. 6 Top view of Launch Complex 39B with azimuthal position of launch towers, and angular ranges where launch towers are downstream of the ML and SLS. The directional rose is centered on the SLS vehicle core stage centerline. Lightning Tower positions are indicated by the red open circles [Source: NASA, Pinier].

Although anemometer sensor output readings provide wind speed and direction directly, data post-processing and

manipulations cannot be performed mathematically using wind direction (Az) and wind speed (V) as variables, but rather using orthogonal vector components. Wind velocity is a 2-dimensional vector with orthogonal components u and v (Westerly and Southerly components, respectively) defined as:

$$u = -V \times sin(Az) \tag{1}$$

$$v = -V \times cos(Az) \tag{2}$$

Conversely, the following equations show how wind direction and speed are calculated from wind velocity components u and v. Wind direction in atmospheric sciences and weather reporting is by convention defined as the direction from which the wind is coming, therefore, it is 180° opposite from the velocity vector pointing direction.

$$V = \sqrt{u^2 + v^2} \tag{3}$$

$$Az = arctan\left(\frac{u}{v}\right) + 180 \tag{4}$$

The anemometers on the LPS record wind data continuously, every day of the year, unless systems are down for maintenance. The 12 sensors provide data files at 1 Hz sampling frequency, as well as 1-minute averages. The analysis in this paper utilizes the one-minute average data files for most of the analyses, and the larger 1 Hz files for dynamic analysis and uncertainty quantification.

In order to illustrate the winds post-processing methodology, from raw LPS anemometer measurements to an estimate of the winds experienced by the vehicle on the launch pad as a function of height, each step is described below and applied to a sample day-long duration of recorded winds on April 7th, 2022 when the SLS was out on the launch pad. Figure 7 shows one-minute average output wind speed and direction from the four anemometers on LT 1 over the whole 24-hour period. The time unit is in Greenwich Mean Time (GMT). Winds that day were categorized as "windy" to "very windy" as they reached a sustained 40 knot wind speed at around 17:30 GMT (only seen in LT 2 and LT 3 measurements). Strong winds result in good signal strength for purposes of demonstrating the methods. In the bottom wind direction plot, the conflicting angular range is highlighted in red and the SLS/ML wake angular range is highlighted in blue. As described previously, when the wind direction is within these ranges, the data are considered unreliable and should be discarded. Figures 8 and 9 show the identical quantities for towers 2 and 3, respectively. It is observed in Fig. 7 that between hours 16:00 and 24:00 winds for LT 1 were in the conflicting range and erratic behavior is noticeable especially on the Level D anemometer (orange curve). Between that same time period, LT 2 wind measurements (Fig. 8) were within the SLS/ML wake range, and a larger wind speed deficit at the lower levels (A, B and C) is observed, indicating that indeed the measurements in the wake of the SLS/ML were corrupted. In comparison, LT 3 measurements (Fig. 9) between 16:00 and 24:00 were well outside of both the conflicting and wake zones, and appear to exhibit normal behavior with winds increasing with height (or Level) and wind direction consistent between levels.

In order to discard data from the two unreliable angular ranges, because the data from a given tower is by definition corrupted, it cannot be used to determine when it actually is in the corrupted ranges. Instead, wind direction from the other two towers is averaged and utilized to estimate when wind direction for the third tower is in one of its own corrupted ranges. Figure 10 shows one-minute averaged raw wind direction measurements for tower pairs at Level D and their averaged wind direction calculated by averaging velocity vector components computed following Eqs. 1 and 2, and converting back to wind direction using Eq. 4. The averaged wind direction for Towers 1 and 2 at Level D (green curve in top plot), for example, is used to determine when the wind direction for Tower 3 at Level D is in one of its corrupted angular ranges. Those data are then discarded. The same operation is applied to the other two towers using the other two averaged pairs, and also applied for all anemometer measurements at the other 3 levels (A, B, and C).

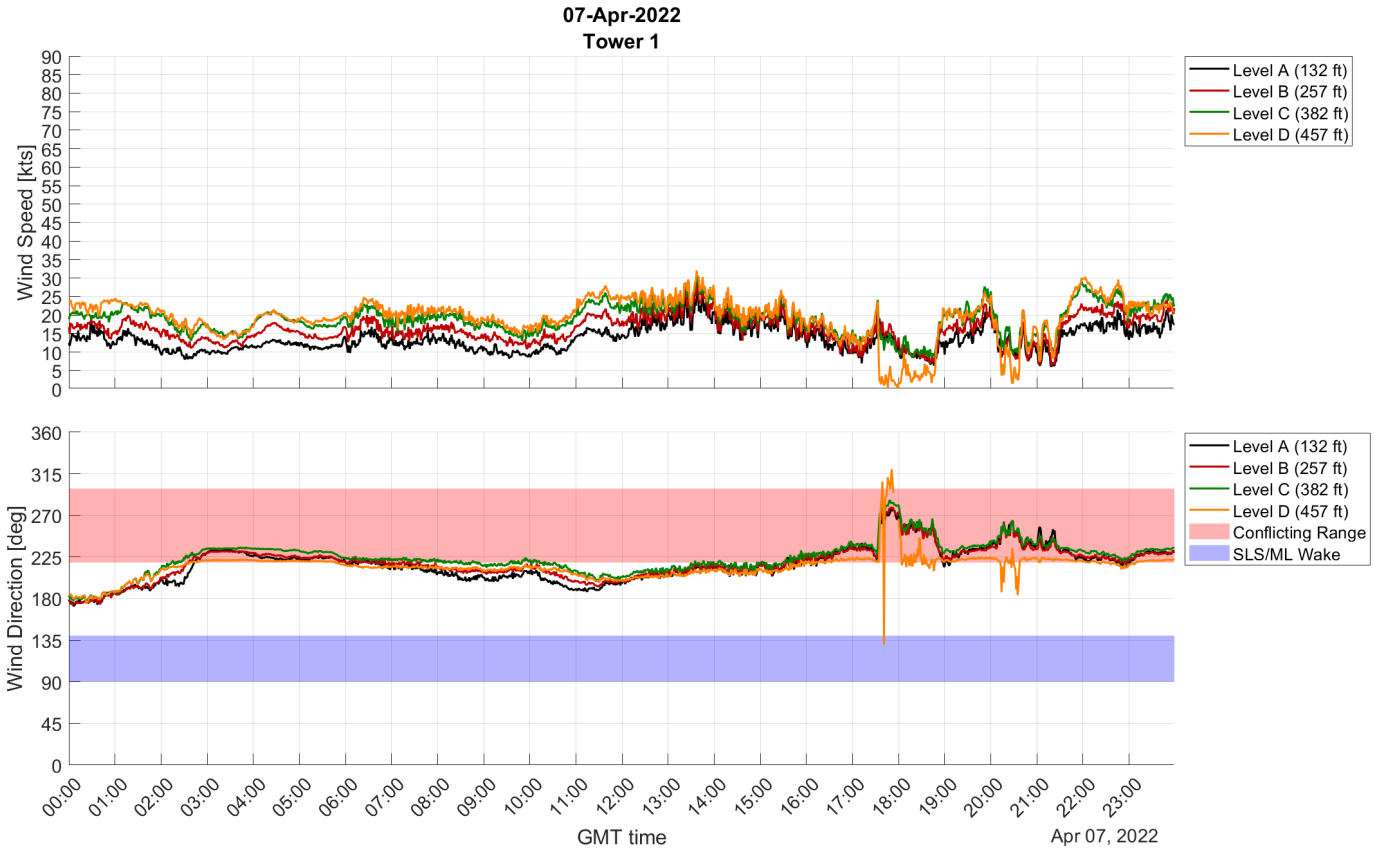

Fig. 7 Wind speed and direction for LT 1 anemometers, April 7, 2022.

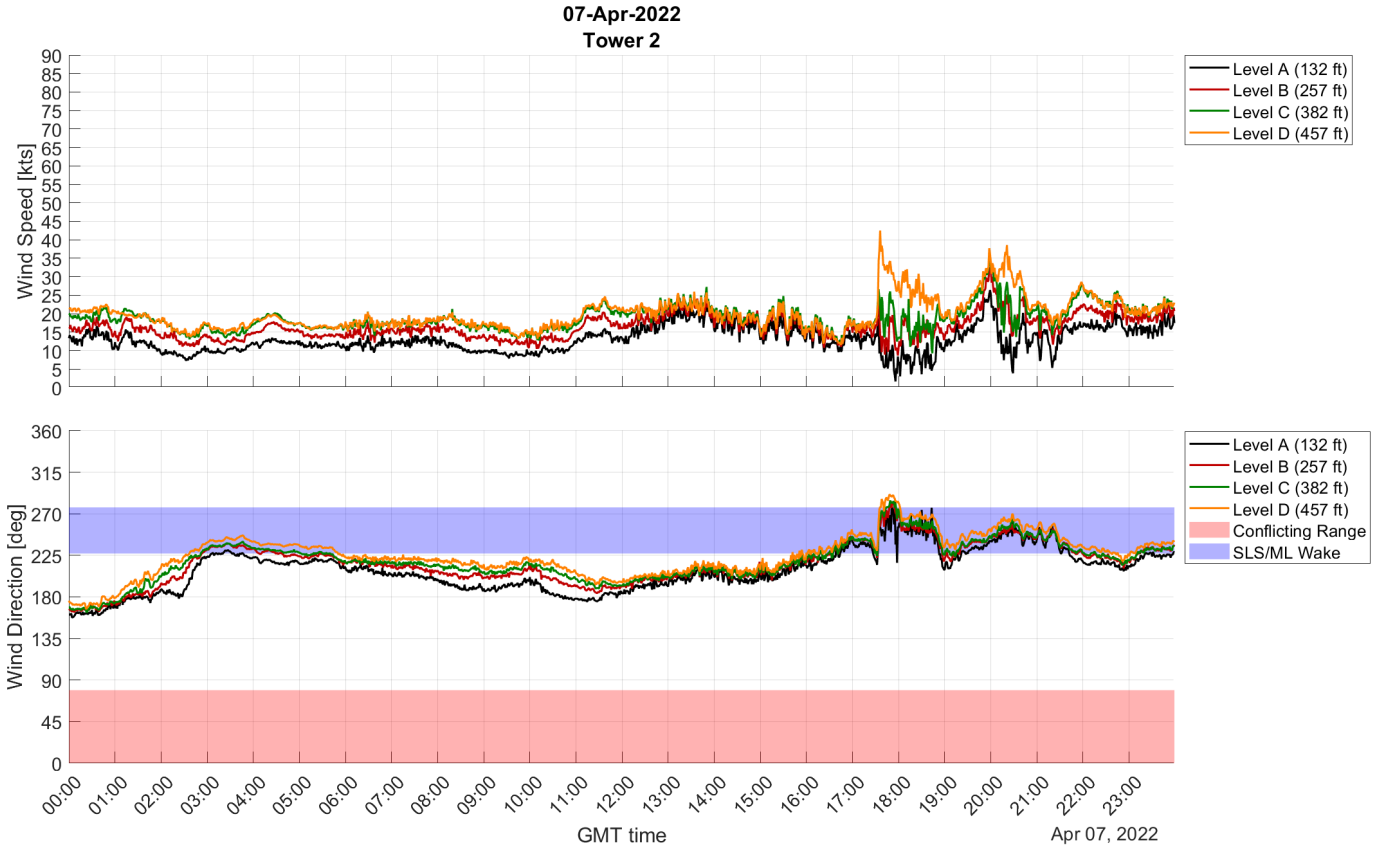

Fig. 8 Wind speed and direction for LT 2 anemometers, April 7, 2022.

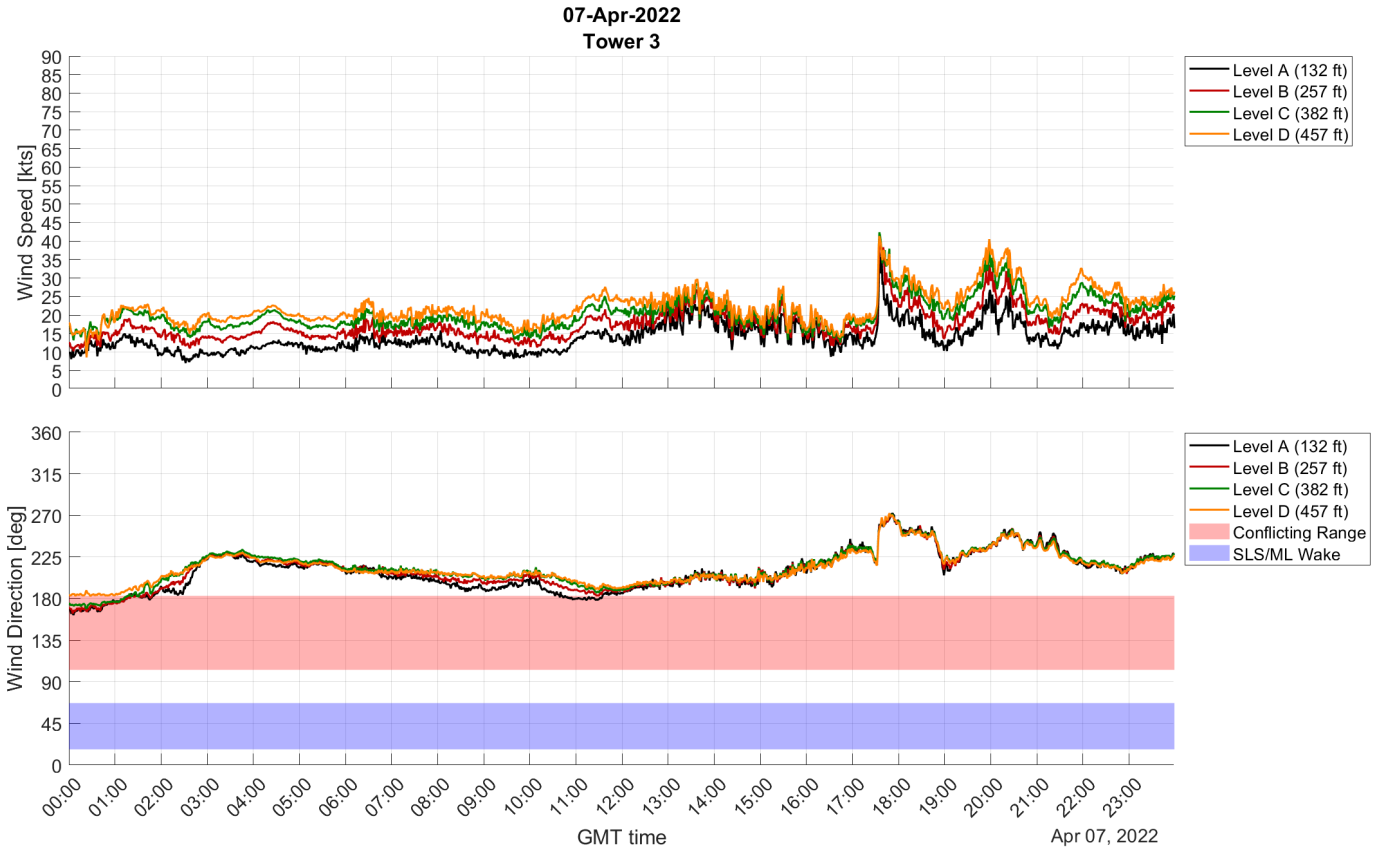

Fig. 9 Wind speed and direction for LT 3 anemometers, April 7, 2022.

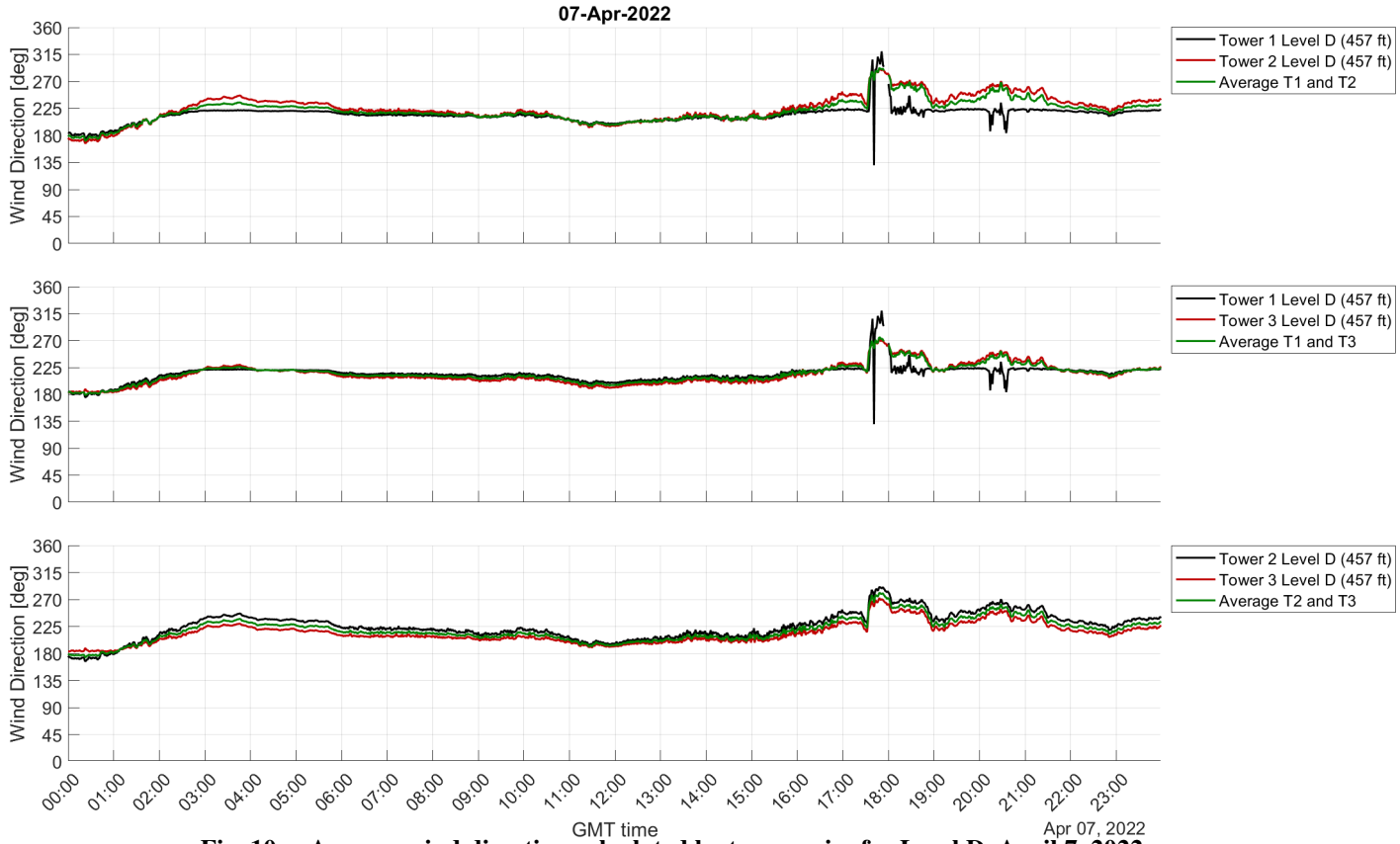

Fig. 10 Average wind direction calculated by tower pairs for Level D, April 7, 2022.

Figure 11 shows the data from anemometers at level D that are considered to be accurate. In this case, on April 7th 2022, the wind speed never dropped below 2 knots, in which case wind direction data would have also been discarded, as they are considered unreliable.

Once all invalid data have been discarded, the final step toward estimating the wind conditions on the launch pad is to average, for each level, the validated anemometer data from the 3 towers. At times, only a single anemometer would provide a valid reading, while at other times, all 3 anemometers at a given level provide valid measurements for this estimation step. As seen in Fig. 11, the time period between 16:00 and 24:00 mentioned previously has a significant amount of data that has been discarded, and thus only one or two anemometers would contribute to the estimated wind speed and direction at the launch pad.

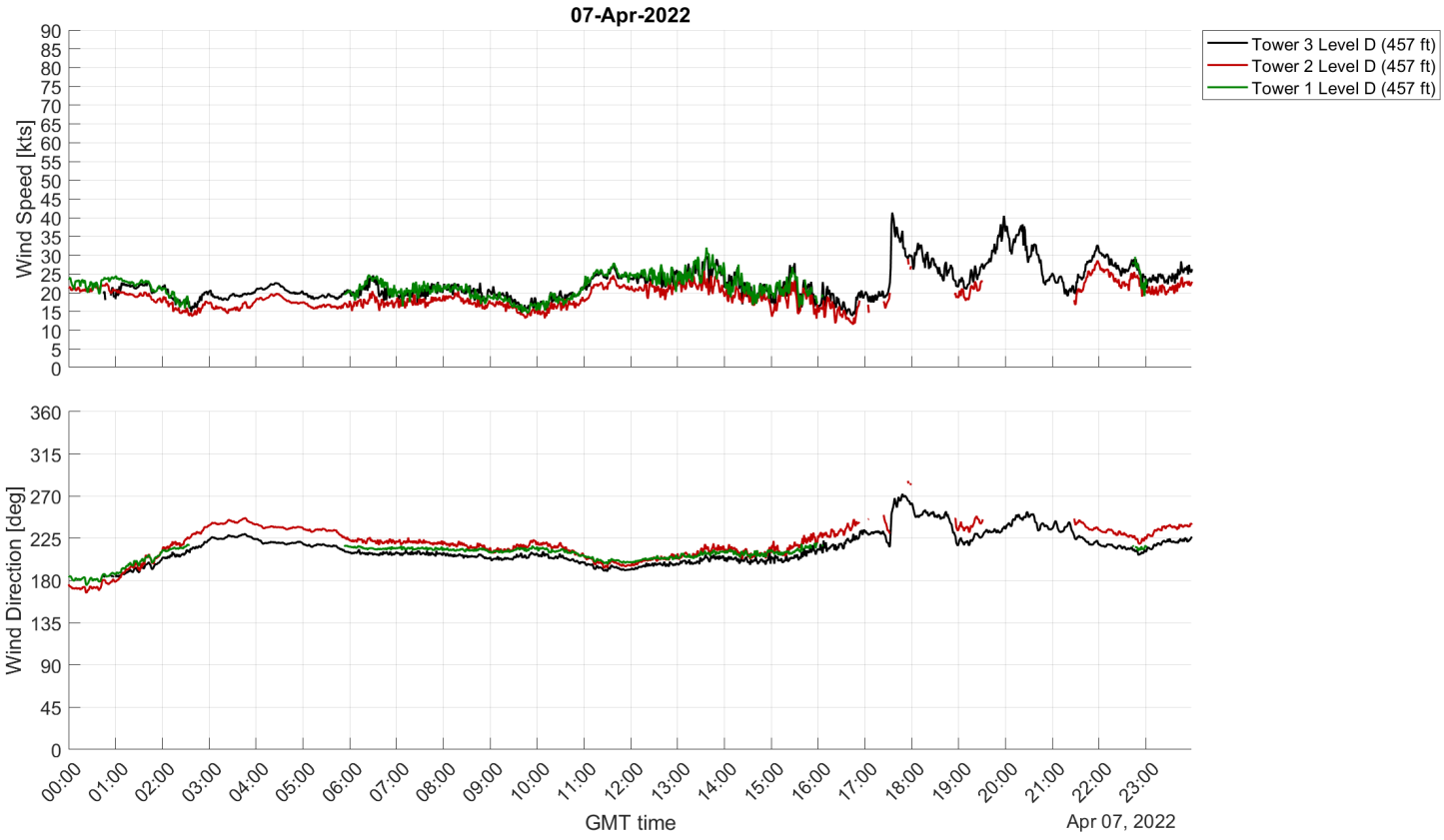

Fig. 11 Validated anemometer data for the three towers at Level D, April 7, 2022.

An estimate of the uncertainty in the wind speed and direction measurements is calculated from two sources of data:

1) The discrepancy between all validated measurements that were utilized to compute the average.
2) The wind speed discrepancy between the one-minute averaged data used as source data for this analysis and the maximum instantaneous wind gust measured during these one-minute windows, as reported in the data files.

The error band at each time step is therefore simply a coverage of the maximum and minimum absolute values observed amongst the above sources of data.

Figure 12 shows the final estimate of the wind speed and direction on the launch pad from all LPS anemometer measurements. This estimate is provided as a function of elevation (4 levels) and now allows correlations of ground winds to measured loads on the pad, which is the topic of ongoing work. The shaded areas around the curves are the uncertainty estimates described above. Note the high wind event that occured at around 17:30 GMT, where sustained winds above 50 kts were observed, which is considered an extreme wind level threat by the National Weather Service,

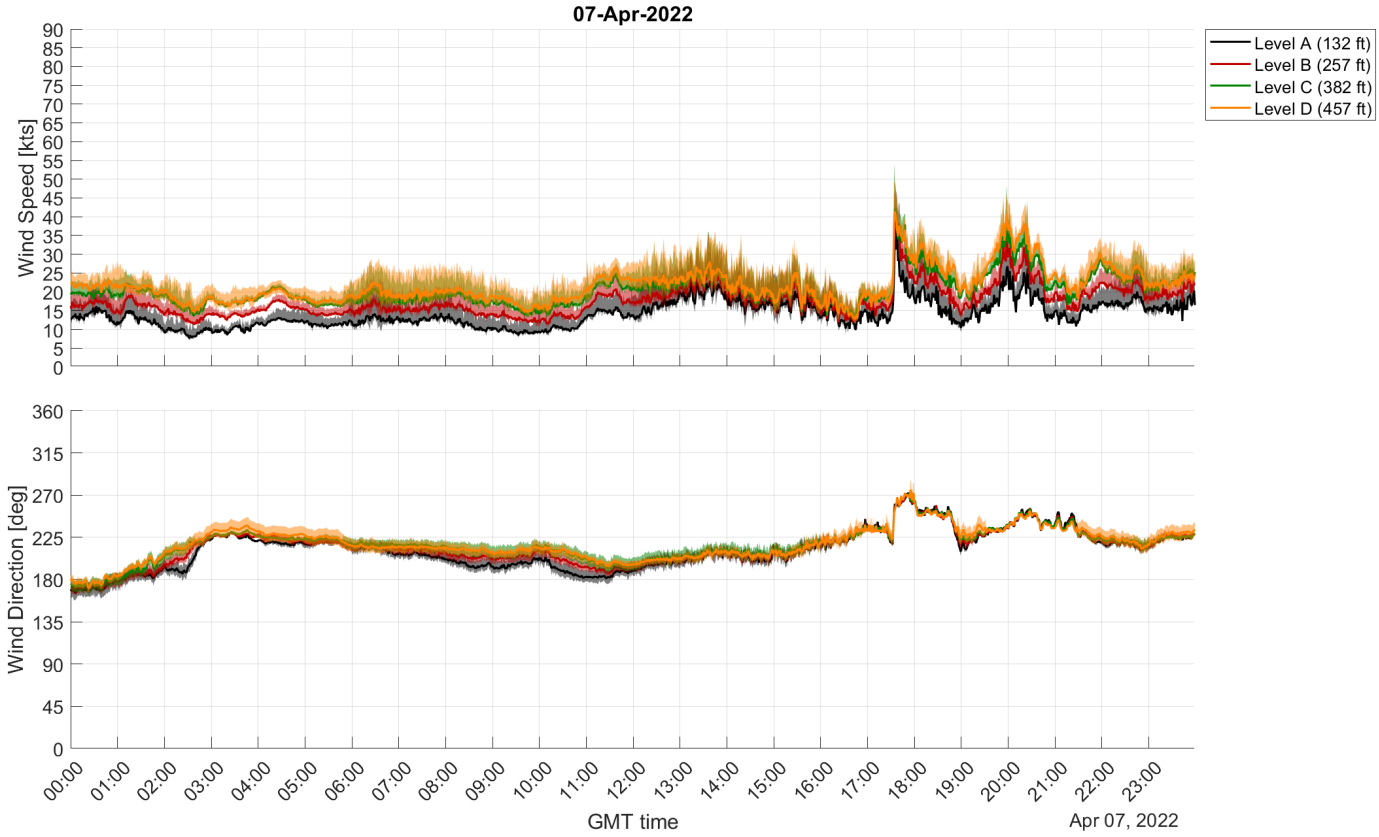

Fig. 12 Wind conditions on the launch pad estimated from all LPS anemometers with error bands in shaded colors, April 7, 2022.

although this wind rapidly weakened in magnitude and no damage to any launch systems were incurred.

High quality, uncorrupted, and undisturbed wind measurements are difficult to implement. There is a high desire to know as best as possible the freestream wind conditions experienced by the large and complex launch system, at all times. However, taking measurements in very close proximity of the hardware can be misleading. For example, the ML has an anemometer installed on the very top of the launch tower. One could assume this would be an ideal place to make such a measurement. However, this specific measurement has proven to be highly unreliable, most likely because the flow presents high curvature around the top of the ML and is most likely very unsteady due to the ML being a highly porous structure with many systems, conduits, and equipment that create an complex flow field in its vicinity. Figure 13 shows smoke flow visualization, as reported in Pinier et al. [3], showing significant curvature of the flowfield above and around the ML and in between the ML and the SLS vehicle. It is clear that any wind measurement taken near the launch system will be unreliable. To support this statement, Fig. 14 shows the post-processed estimates of launch pad winds shown previously, along with the anemometer measurement from the top of the ML (in blue). It is very clear that this is an unreliable measurement as it shows significant unsteadiness in both speed and wind direction, and very large errors compared to the high fidelity post-processed LPS winds. The full extent of the reasons for these discrepancies is so far unknown, but this ML measurement is not being used for any analysis at this point due to its corrupted nature.

Fig. 13 Smoke flow visualization of a scaled liftoff SLS Block 1B crew vehicle model and the mobile launcher. Flow direction is indicated by the blue arrows [Source: NASA].

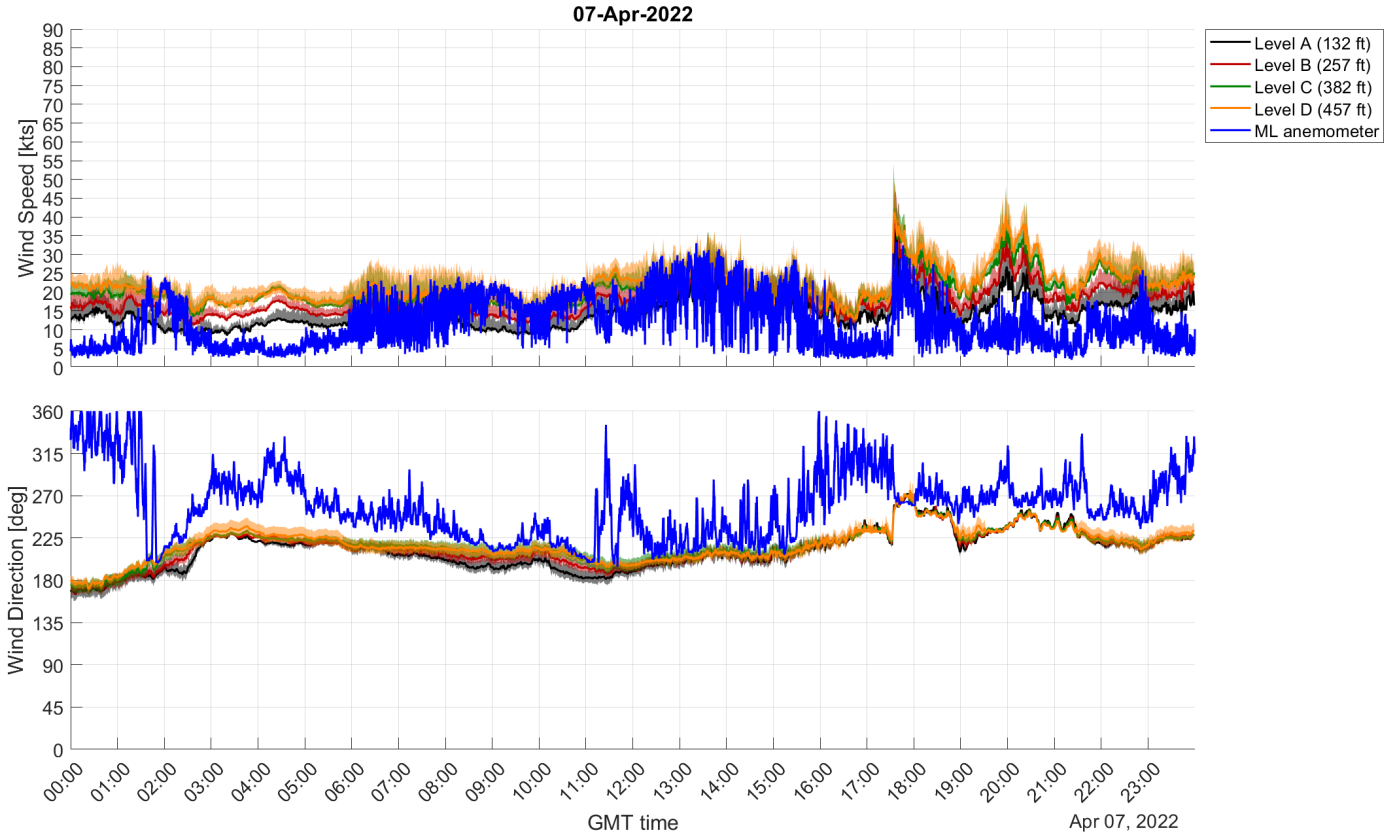

Fig. 14 Wind conditions on the launch pad estimated from all LPS anemometers with raw ML anemometer measurement, April 7, 2022.

The next section provides an overview of the nature of the winds the SLS vehicle experienced while sitting for a number of days on the launch pad for the Artemis I mission, exposed to the Florida weather in 2022.

IV. Artemis I: SLS On-Pad Stays and Significant Wind Events

The Artemis I mission was the first test flight of the SLS rocket, and therefore, the first full test of all ground support systems required to fully prepare a large deep space rocket for launch, including liquid hydrogen and liquid oxygen supply and tanking infrastructures, nitrogen gas purge and water deluge lines, and many other critical systems both on the ground and on the vehicle. Fully tanking such a large cryogenic fueled rocket is a great challenge. It thus unsurprisingly took a few attempts to complete a Wet Dress Rehearsal (WDR), and a few launch attempts to have all systems behave nominally until terminal count and liftoff at T=0. The total amount of time the rocket and mobile launcher spent on the launch pad as teams worked through these tests was much greater than what it would normally be. During those periods of time between March and November of 2022, the rocket was exposed to many days of Florida weather, including 12 high wind days and Hurricane Nicole. Table 2 is a summary of all four separate periods of time the SLS and ML were on the launch pad, with fuel tanks empty for a majority of that time, along with the list of major launch preparation events that occurred, and all the days considered to have high winds. According to the National Weather Service, a high wind threat level is defined as: "A high threat to life and property from high wind, with sustained speeds of 40 to 57 mph (or 35 to 50 kts)." A few of the days had sustained winds higher than 50 kts, which is considered an "Extreme level wind threat".

Table 2 Summary of on-pad stay periods for the SLS and ML before the Artemis I mission. All winds speeds are at Level B (257 ft).

Rollout Count	Dates and Duration	Major Events/Tests	High Wind Days, Max wind speed
1	03/17/22 to 04/25/22 40 days	WDR 1 (04/03) WDR 2 (04/04) WDR 3 (04/11)	03/19/22, 37.9 kts 03/24/22, 40.9 kts 03/31/22, 38.2 kts 04/02/22, 48.5 kts 04/07/22, 54.2 kts 04/09/22, 43.7 kts
2	06/06/22 to 07/02/22 27 days	WDR 4 (06/20)	06/06/22, 47.2 kts 06/10/22, 38.5 kts 06/18/22, 46.7 kts
3	08/17/22 to 09/27/22 42 days	Launch Attempt 1 (08/29) Launch Attempt 2 (09/03) Full Tanking Test (09/21) Rollback for Hurricane Ian	08/17/22, 44.4 kts 08/20/22, 38.5 kts 09/08/22, 41.0 kts 09/09/22, 39.1 kts 09/10/22, 62.4 kts 09/12/22, 47.8 kts
4	11/04/22 to 11/16/22 12 days	Artemis I Launch (11/16)	11/09/22, 59.5 kts (Hurricane Nicole) 11/10/22, 81.0 kts (Hurricane Nicole) 11/11/22, 39.1 kts (Hurricane Nicole)

The SLS/ML system was on the launch pad for a total of 121 days, all of which have continuously recorded wind measurements from all LPS anemometers. One of the interesting high wind events that occurred was on June 6th, 2022, on the day of the second rollout of SLS to the pad (see Table 2). Figure 15 shows the post-processed wind speeds and directions estimated at the launch pad for the whole day. Rollout occurred between approximately 05:00 and 15:00 GMT during a very low wind time period (under 10 kts). But at 21:00 GMT, after winds from the East (90°) steadily increased in strength, the wind direction suddenly, over the course of minutes, shifted to the Northerly direction (0° or 360°) and dropped in magnitude, then suddenly, within minutes, increased to a sustained 30 to 45 kts for at least 30 minutes before it suddenly died down and shifted back to an Easterly direction. This type of strong but short lived (1 hour) high wind event was found to have occurred at least 9 times over the course of the 12 days. The Appendix at the end of this paper shows plots of winds for all 18 days (out of 121 on the pad) that exposed the vehicle to high or extreme winds, as shown in the last column of Table 2. It is informative to analyze the types of ground wind forcing our launch vehicle and ML can encounter in real conditions, in order to help us make better predictions of the types of forcing our Artemis II vehicle might encounter in preparation for our next flight, and to provide an input for evaluating whether combined loads analyses models correlate well with recorded wind forcing and measured strain gauge responses on various parts of the launch vehicle.

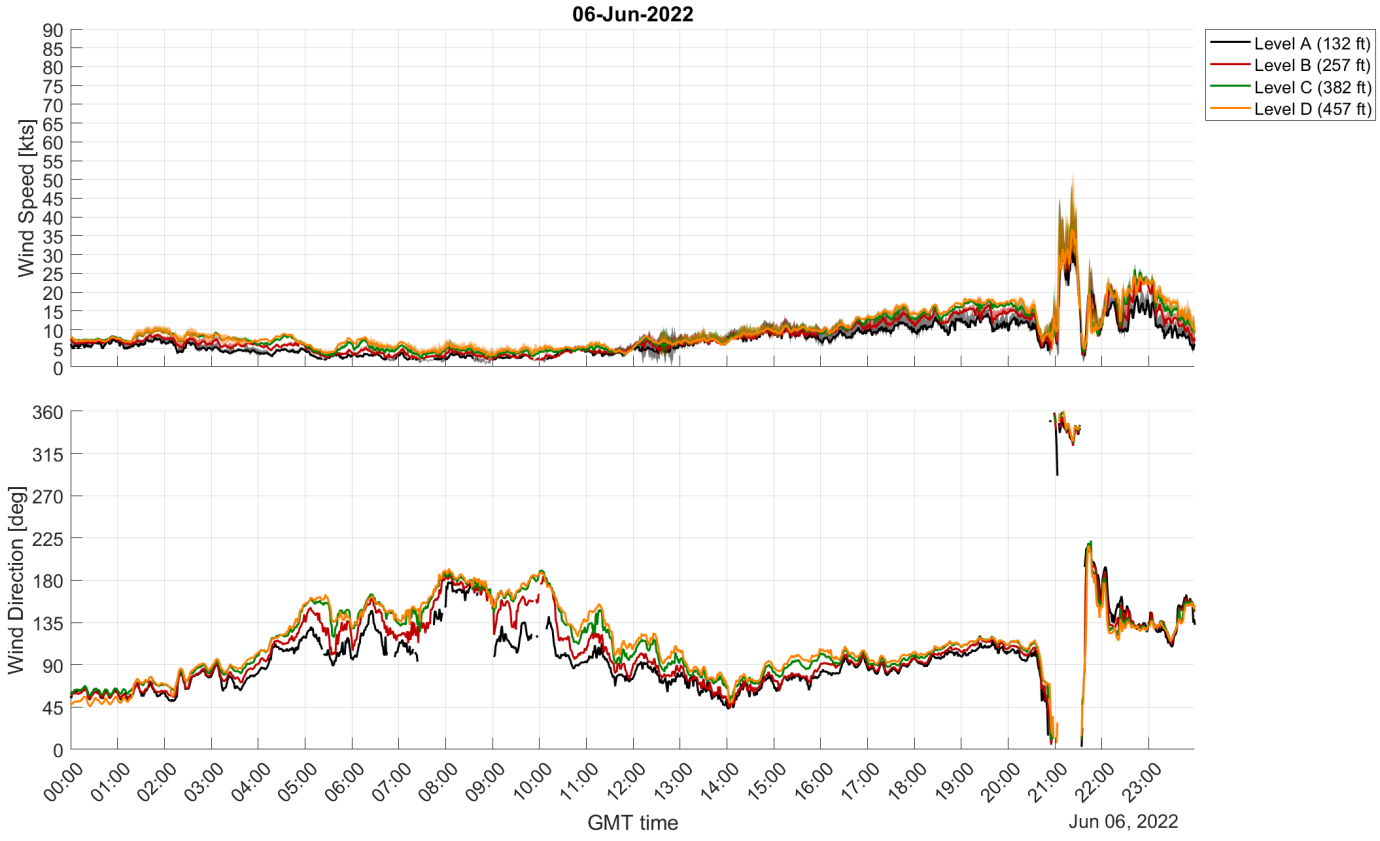

Fig. 15 Wind conditions on the launch pad estimated from all LPS anemometers, June 6, 2022.

During the period of time the vehicle was out on the pad before the Artemis I launch, two tropical storms formed in the Caribbean Sea and Atlantic Ocean and were predicted to take a path in the general direction of Florida and Cape Canaveral. Figures 16 and 17 show the initial predicted paths of both Tropical Stroms. Accurate predictions of tropical storms and hurricane paths are very difficult, especially days away from making landfall. In both cases, a difficult decision had to be made by the Artemis I Mission Management Team (MMT) as to whether to rollback the launch vehicle and ML to the VAB, or stay on the pad in a safe and secure configuration. Rollbacks are a complex operation. They take a tremendous amount of time and effort, and the structural vibrations endured by the rocket during rollout and

rollback trips on the crawler-transporter adds measurable wear and tear on the hardware, which is not desirable and limits the lifespan of the launch hardware. Based on all the data available several days before the potential hurricane landfall, rollback decisions had to be made. The MMT decided to rollback on 09/27/2022 before Tropical Storm Ian made landfall from the West, and decided to stay out around 11/08/2022 and ride out Tropical Storm Nicole as it made landfall from the East. A retrospective look at the actual winds recorded by the LPS anemometers during both storms is presented here, and shows that the Nicole winds at Cape Canaveral ended up being much more significant than during Ian. In hindsight, staying out on the pad during Ian would have been most likely safe, and rolling back before Nicole might have been a safer choice if the team had known the unusually strong and sustained winds that were going to be experienced. Figures 18 and 19 show post-processed wind speeds and direction for Ian and Nicole, respectively. Note that the maximum wind speed during Nicole was measured around 9:00 GMT with a speed of 85 kts at the highest level of the LPS (457 ft), while Tropical Storm Ian's maximum winds only reached 55 kts at the highest level of the LPS. Despite being very strong, these winds encountered by the vehicle on the pad are within our design limits for the integrated system.

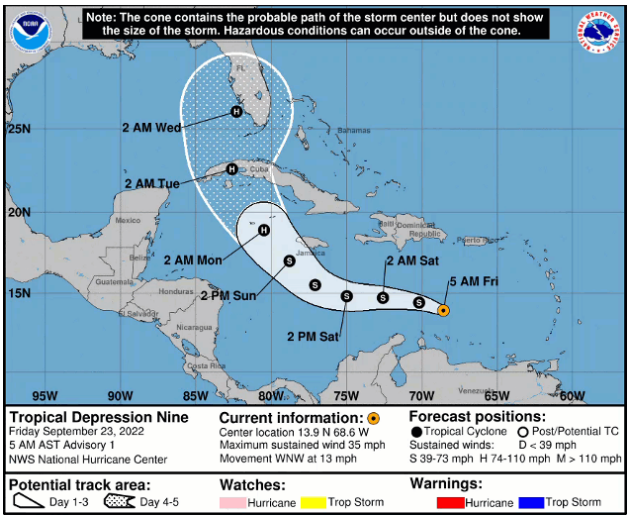

Fig. 16 Early predicted path with cone of uncertainty of Hurricane Ian that hit Florida during Artemis I prelaunch operations. Credit: NOAA National Weather Service.

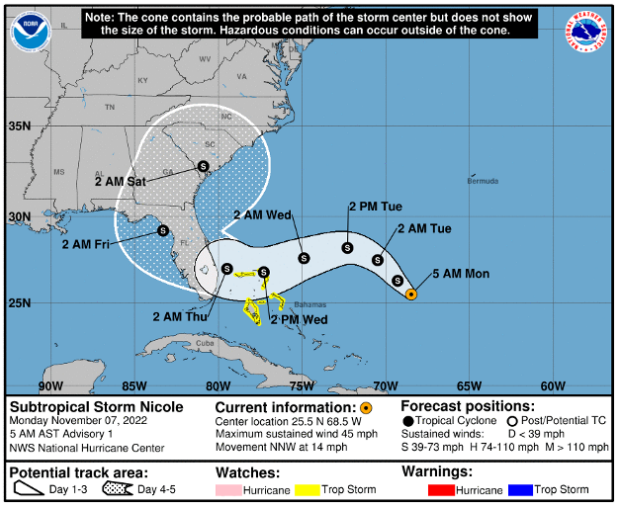

Fig. 17 Early predicted path with cone of uncertainty of Hurricane Nicole that hit Florida during Artemis I prelaunch operations. Credit: NOAA National Weather Service.

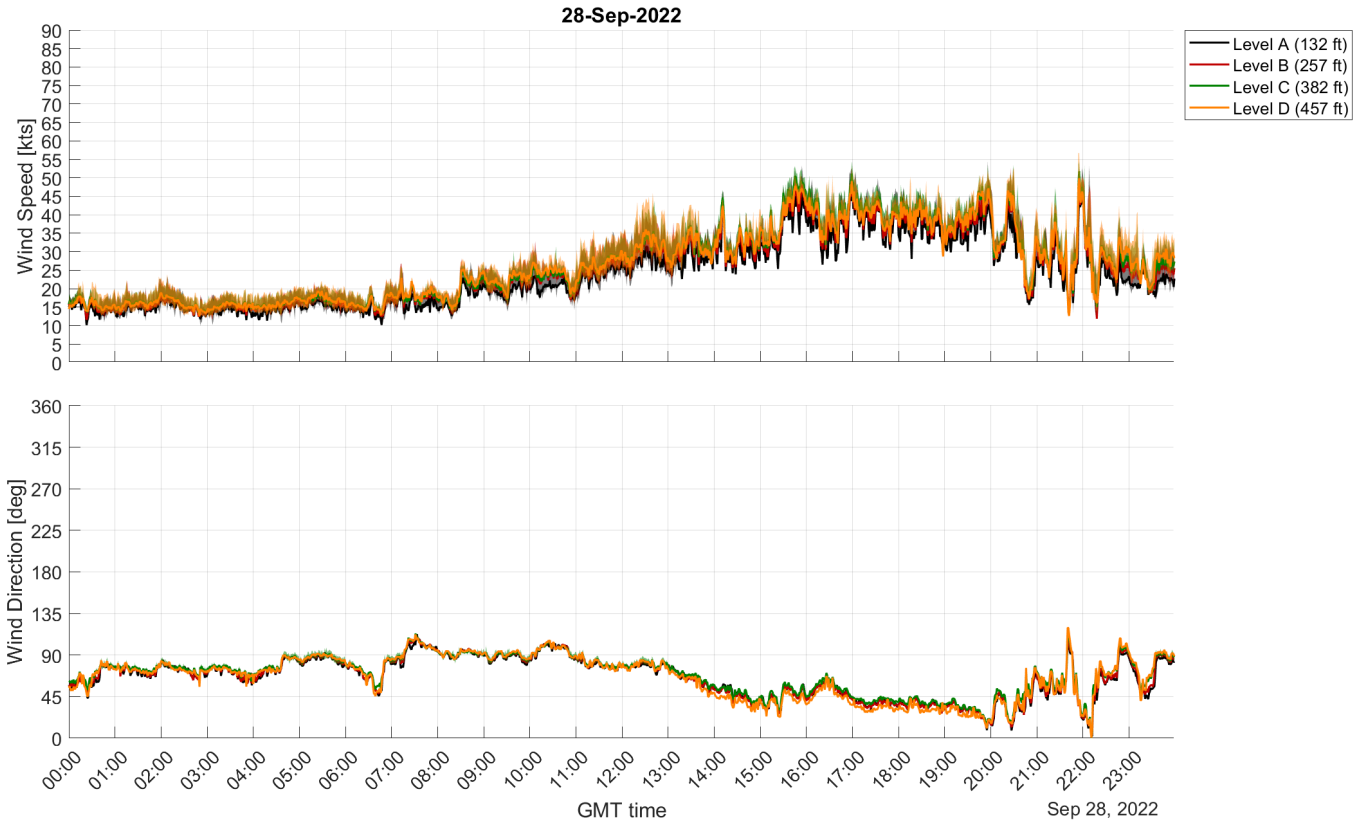

Fig. 18 Wind conditions on KSC launch pad 39B estimated from all LPS anemometers during Tropical Storm Ian, September 28, 2022.

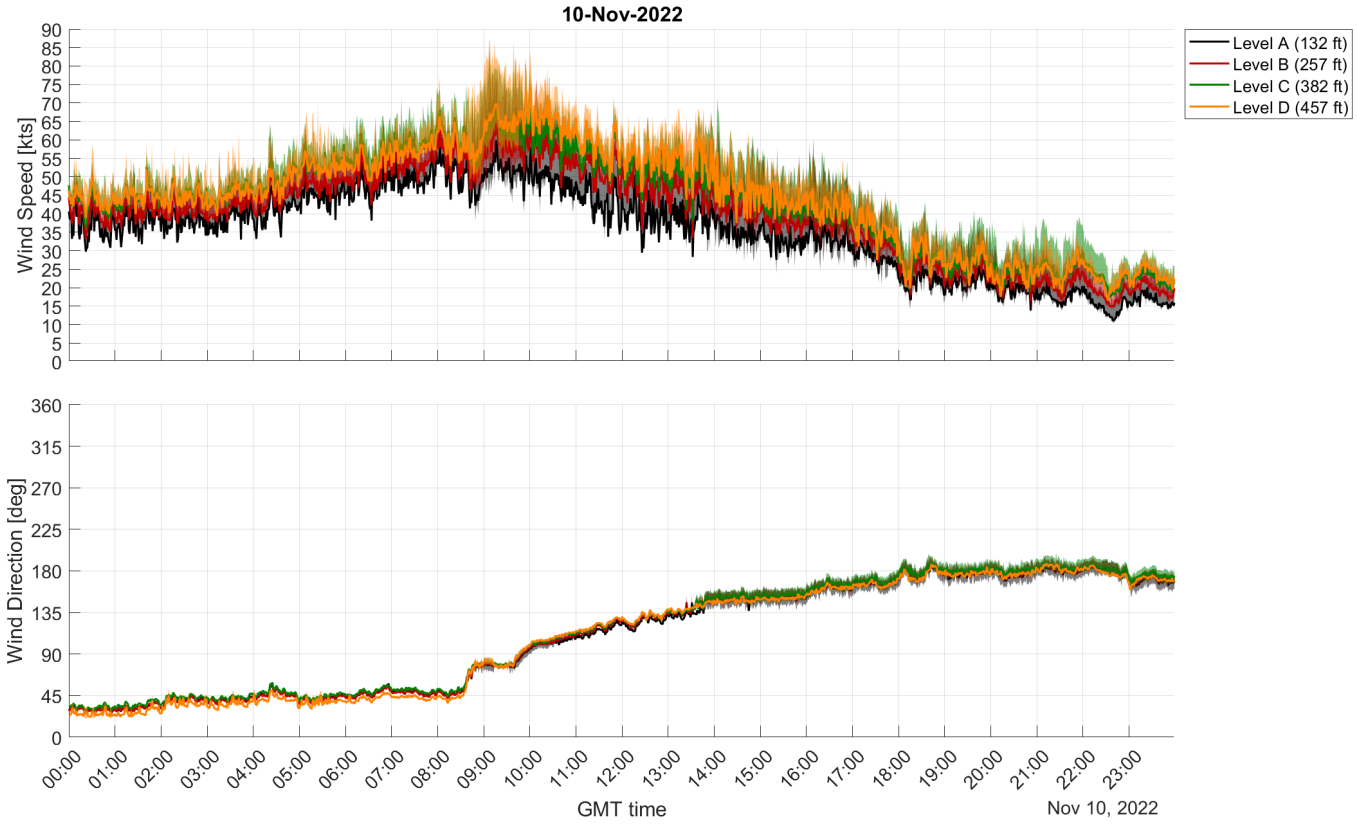

Fig. 19 Wind conditions on KSC launch pad 39B estimated from all LPS anemometers during Hurricane Nicole, November 10, 2022.

In order to design launch vehicles and other space systems, like many developed by the NASA Exploration Systems Mission Directorate along with other commercial partners, NASA has derived and made public a Cross-Program Design Specification for Natural Environments (known as the DSNE [13]). This document defines the natural environments characteristics and quantities to be used by all Exploration Programs. Many of these parameter limits and characteristics (model-based, statistical, empirical) are based on experience with previous programs, such as the Space Shuttle Program. Natural environments include terrestrial, space, and destination environments (Moon, Mars, asteroids, etc). One of the terrestrial environments is the "Ground Winds for Transport and Launch Pad Environments" (defined from 0 to 492 ft altitude), which should be used as maximum design limits for hardware that will be exposed to these winds during ground operations at KSC, like the SLS and ML. The following analysis shows how these predefined design environments compare to some of the strongest winds that the vehicle and ML experienced during Hurricane Nicole.

The 3-sigma statistical peak wind-speed profile is defined in the DSNE as follows:

$$u(z) = u_{18.3}\left(\frac{z}{18.3}\right)^{1.6(u_{18.3})^{-3/4}} \tag{5}$$

where $u(z)$ is the peak wind (in meters per second) at height z (in meters) and $u_{18.3}$ is the peak wind speed (in meters per second) at 18.3 m altitude.

As described in Collins et al. [6], there are four pre-defined operational phases that provide a value for $u_{18.3}$ that is a function of the duration of the phase. The longer the duration (in days or hours), the higher $u_{18.3}$ will be and the stronger the wind profile as provided by Eq. 5 are. The four operational phases with their pre-defined $u_{18.3}$ values are:

1) Transport To/From Pad, $u_{18.3} = 30.8\ m/s$
2) On-Pad Unfueled, $u_{18.3} = 38.3\ m/s$
3) On-Pad Intermediate and Fully Fueled, $u_{18.3} = 24.2\ m/s$
4) Vehicle Launch, $u_{18.3} = 17.7\ m/s$

Because the "On-Pad Unfueled" phase can be by far the longest in duration, it has the strongest design peak wind profile requirement. This is the wind profile that is applicable to all 121 on-pad stay days that were reported in this article, until a few hours before wet dress rehearsals or launch events when core stage fueling starts and the design winds shift to the third phase described above. From the peak wind profiles, the DSNE describes how the steady state wind profile is calculated:

$$\overline{U}(z) = u(z)\left(1 + \left(\frac{\left(\frac{18.3}{z}\right)^{0.283-0.435e^{-0.2u_{18.3}}}}{1.98 - 1.887e^{-0.2u_{18.3}}}\right)\right)^{-1} \tag{6}$$

where $\overline{U}(z)$is the steady state wind (in meters per second) at height z (in meters), $u(z)$ is the peak wind (in meters per second), and $u_{18.3}$ is the peak wind speed (in meters per second) at 18.3 m altitude.

Figure 20 shows a vertical representation of the peak winds over one minute (black vectors) along with the one-minute average winds (red vectors) as measured by the 12 anemometers and post-processed using our methodology, for a specific time of 9:59 GMT during the Hurricane Nicole event. Figure 19 shows that this would be near the strongest part of the storm. The faded color vectors indicate the maximum peak wind measured during a 2-hour time period from 10:00 to 12:00 GMT. It is observed that despite the very strong winds experienced, there was still a healthy design margin at every altitude during this time period, and the wind speed deficit with lower altitude is clearly shown and correlates well with the DSNE-defined peak (black) and steady state (red) winds. A scan of each individual minute of wind measurements during the entirety of the storm portrays an observation consistent with the above, with winds gradually increasing with altitude, but always staying uniformly below the peak wind design profile.

The instantaneous wind estimation methodology presented in this paper was not yet developed during Artemis I operations, and raw anemometer readings were utilized directly to assess real-time winds, despite some measurements being corrupted for certain wind directions and intensities. The intent is to now develop in preparation for Artemis II, a real-time graphical user interface compatible with the launch support software environment that would calculate in real time the estimates of launch pad winds based on direct anemometer measurements. More accurate assessments of

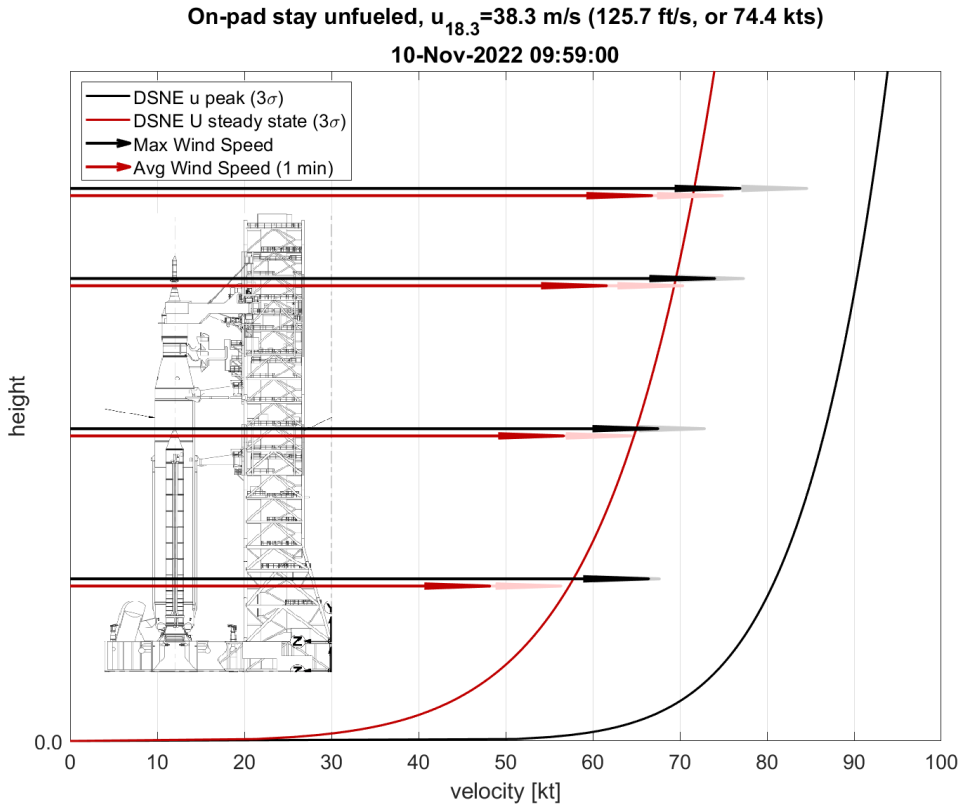

Fig. 20 Vertical representation of maximum (black arrows) and average (red arrows) winds over one minute at 9:59 GMT during Hurricane Nicole, on November 10, 2022, with DSNE peak and steady state wind design profiles. Light shaded arrows are the maximum peak and steady state winds over a 2-hour window.

vehicle winds experienced and better correlations with measured loads on the pad could be performed. This would then feed into better informing the decision process for rollout and rollback calls.

V. Future Work

The next natural step in this analysis is to utilize the more accurately derived launch pad wind estimates presented in this paper to calculate full-scale vehicle aerodynamic coefficients using strain gauge and direct load measurements collected on the vehicle and the ML, assuming a center of pressure location that could be provided by past wind tunnel tests [4][6][7]. These full-scale aerodynamic coefficients can then be compared to wind tunnel based aerodynamic databases to provide correlations between scaled ground tests at reduced Reynolds numbers, and full-scale vehicle measurements. It is to be expected that full-scale measurements at only four individual altitudes will always be less accurate of an input freestream flow condition, and any estimates of full-scale aerodynamic coefficients would be associated with higher uncertainties. However, this will provide a first full-scale estimate of aerodynamic coefficients for ground winds based off these high quality post-processed wind measurements, and will provide a large dataset of direct full-scale Reynolds number measurements that could be probed for physical flow phenomena like the Coandă effect, or biased flow attachment in downstream regions of the vehicle, that was observed both during ground testing and CFD simulations [8]. Such a dataset will be a unique grounding tool for making future ground test data more representative of reality.

VI. Conclusion

From our successful first launch of the SLS rocket during the Artemis I mission, the teams across the NASA Centers have learned many great lessons, and have been working hard to improve on them to make the Artemis II mission even more successful, taking this time a crew of four astronauts (Christina Koch, Victor Glover, Jeremy Hansen, Reid Wiseman) further into space than humans have ever been before. On the flight data analysis side, we have shown in this paper, and were reminded that real flight data is nontrivial to post-process because it is imperfect, at times can be corrupted, affected by "real world" constraints (e.g., instruments or sensors break and are difficult to repair, power outages), which can often result in missing data or worse: misleading data (data that are not clearly corrupted but inaccurate). It is difficult to overstate how noisy and uncertain flight data can be, and therefore, extra care and caution need to be implemented when handling such data. An effort to estimate some level of uncertainty in the flight data is required to ensure that the reader is not misled into believing flight data have a higher level of accuracy than they actually do, especially when correlating and comparing to ground test data, which usually will have much smaller uncertainties due to a very controlled environment and input or boundary conditions. This work has enabled a better understanding and validation of what wind conditions (often high winds) that the rocket and mobile launcher actually experienced on the launch pad for 121 days before the Artemis I launch. This experience and collection of ground wind forcing data on the rocket could help inform the decision making for the next launch readiness for the Artemis II mission, in case of exposure of the vehicle to severe or high risk weather events. This would minimize the uncertainty in any flight rationale development that would include estimates of actual wind loads experienced by the vehicle due to weather.

Appendix:

All post-processed high or extreme wind days with SLS/ML on Launch Pad 39B

Figures 21 through 38

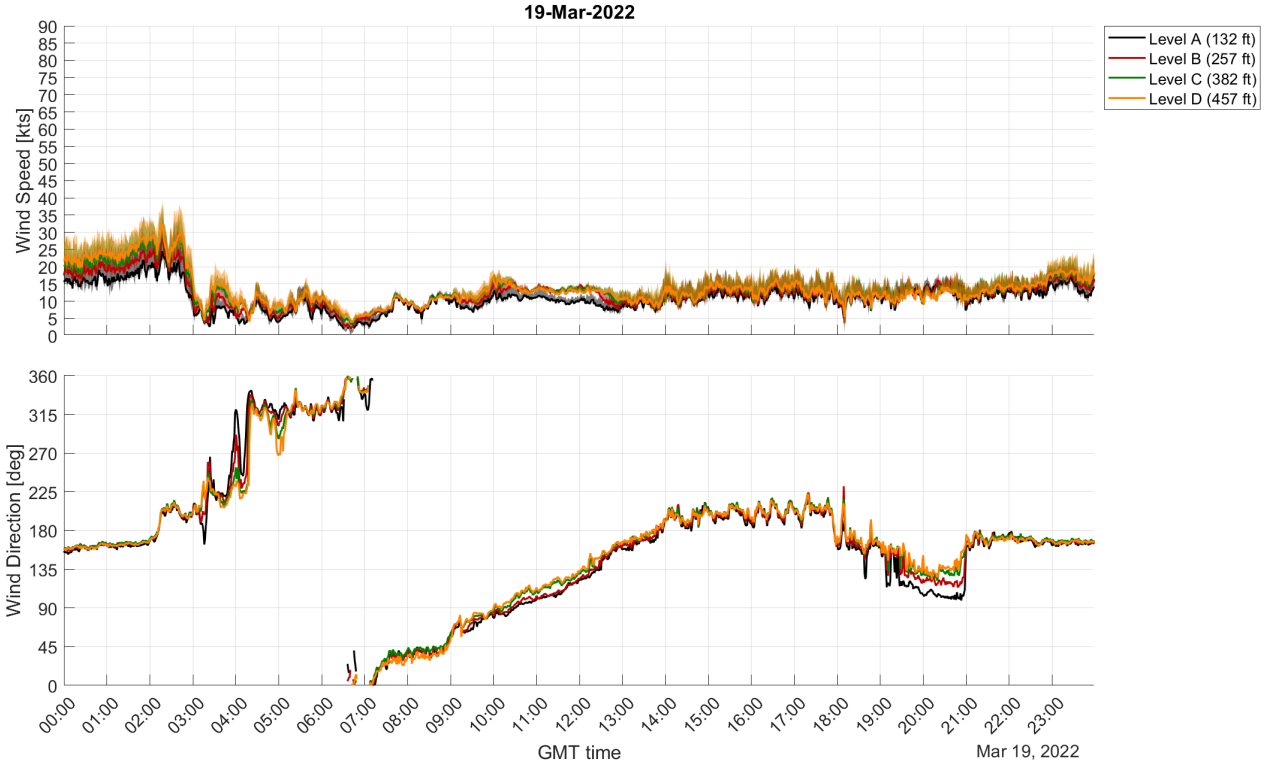

Fig. 21 Estimated wind speed and direction on the launch pad, March 19, 2022.

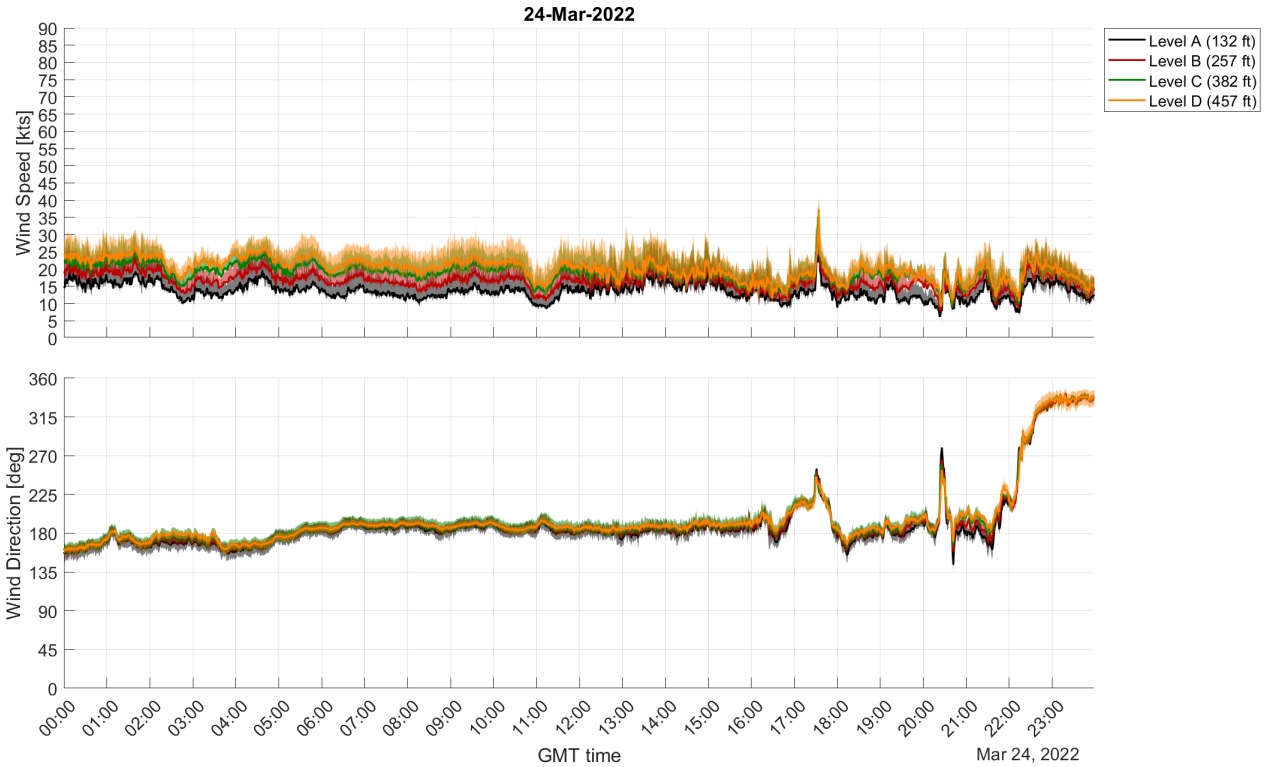

Fig. 22 Estimated wind speed and direction on the launch pad, March 24, 2022.

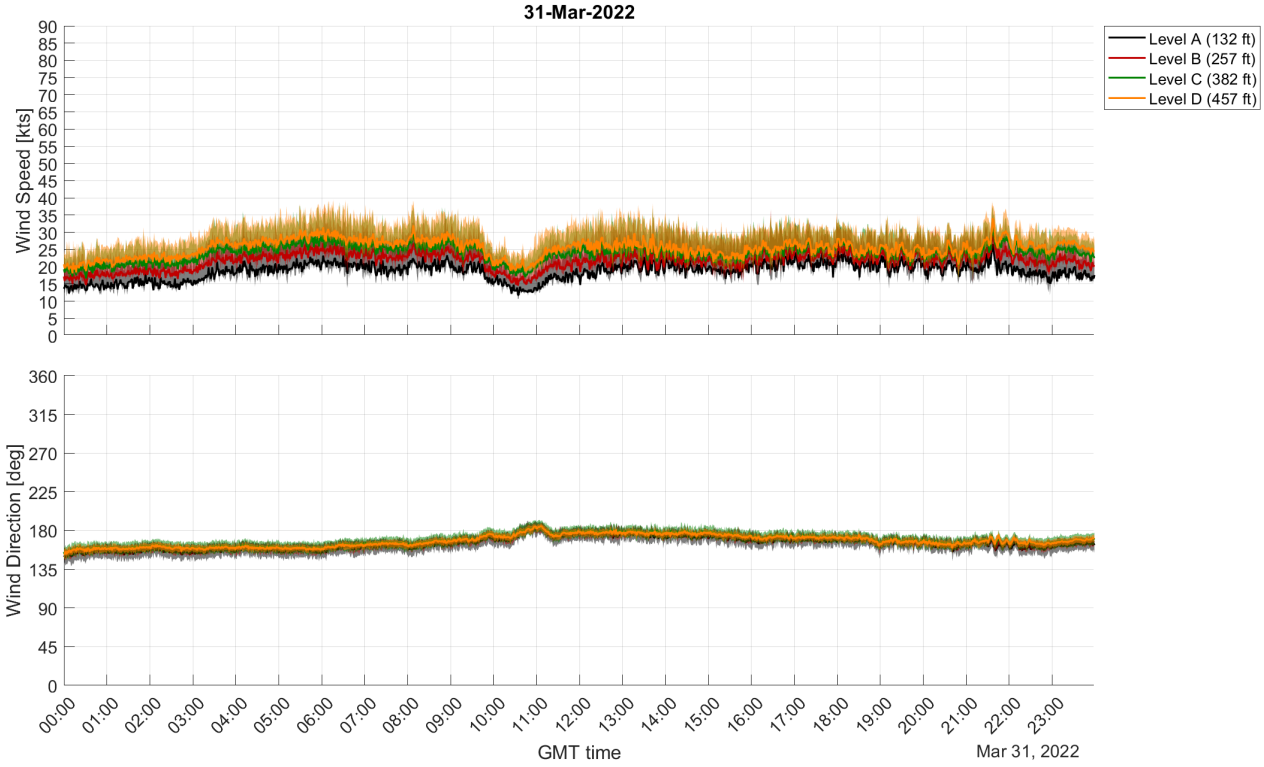

Fig. 23 Estimated wind speed and direction on the launch pad, March 31, 2022.

Fig. 24 Estimated wind speed and direction on the launch pad, April 2, 2022.

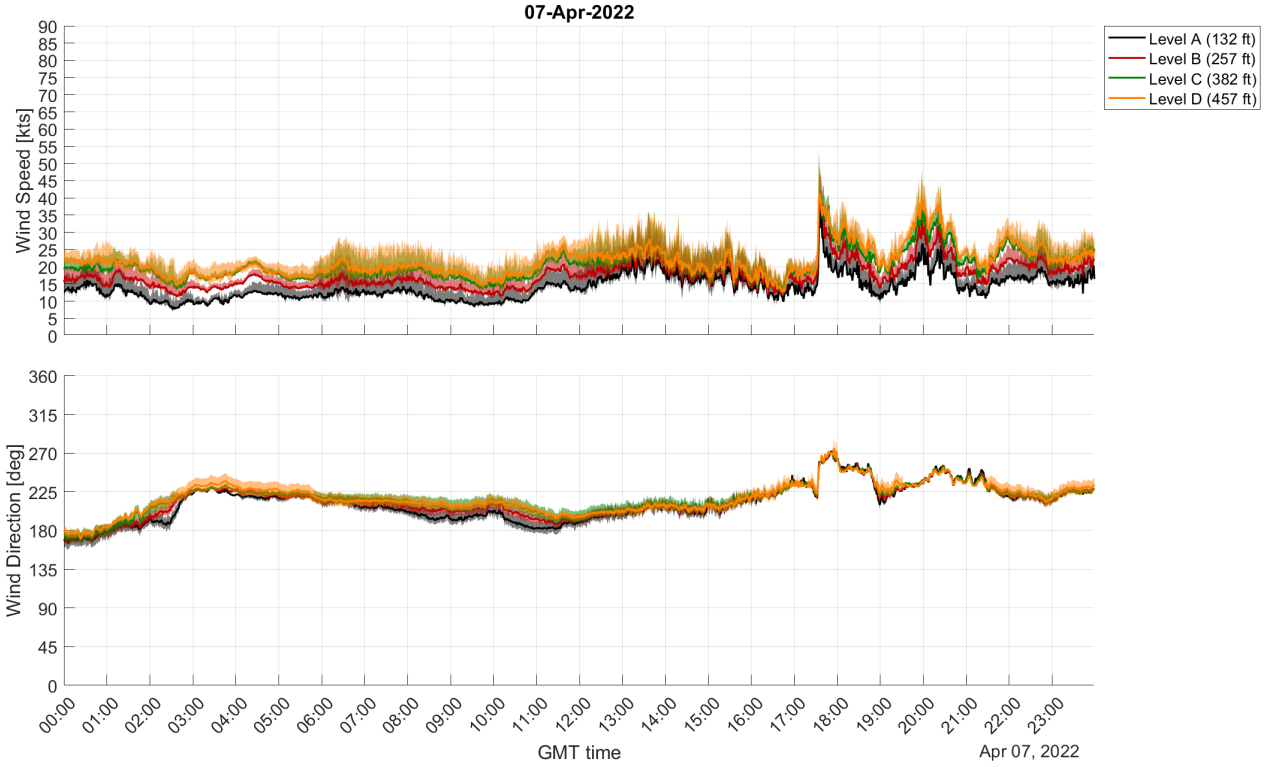

Fig. 25 Estimated wind speed and direction on the launch pad, April 7, 2022.

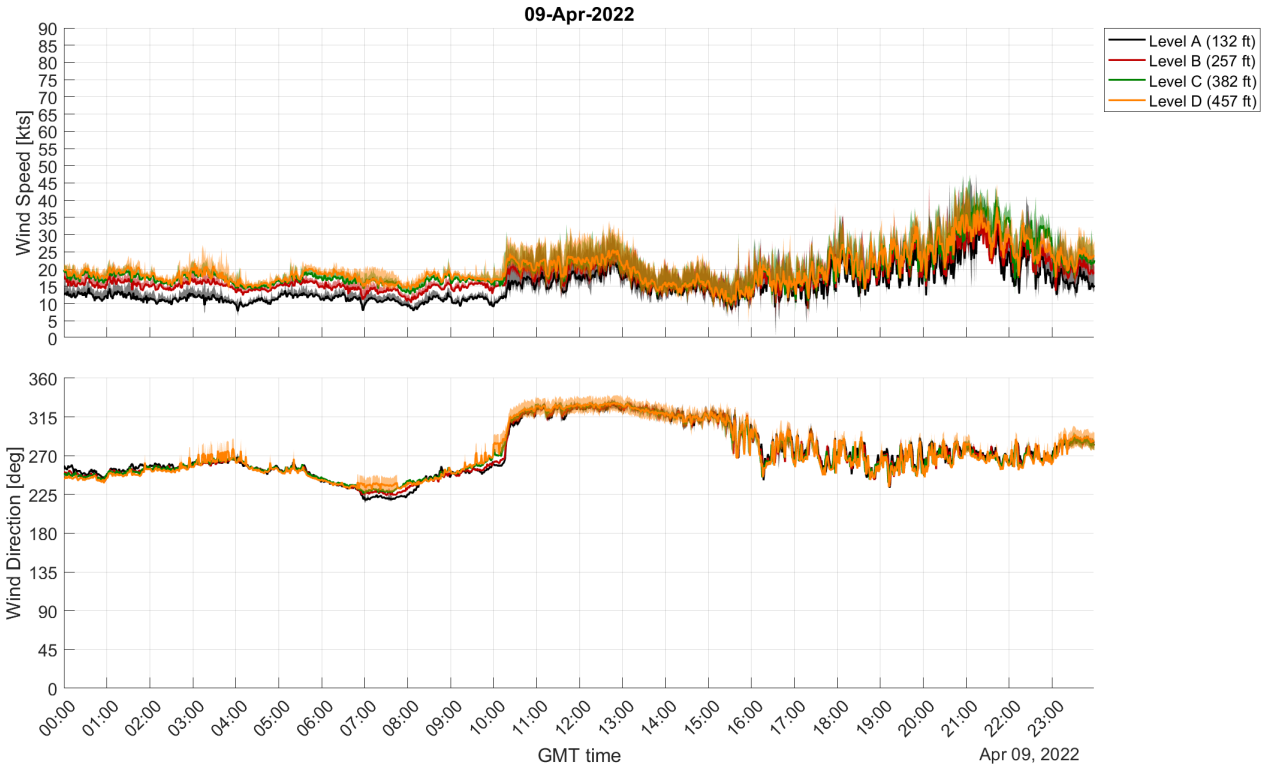

Fig. 26 Estimated wind speed and direction on the launch pad, April 9, 2022.

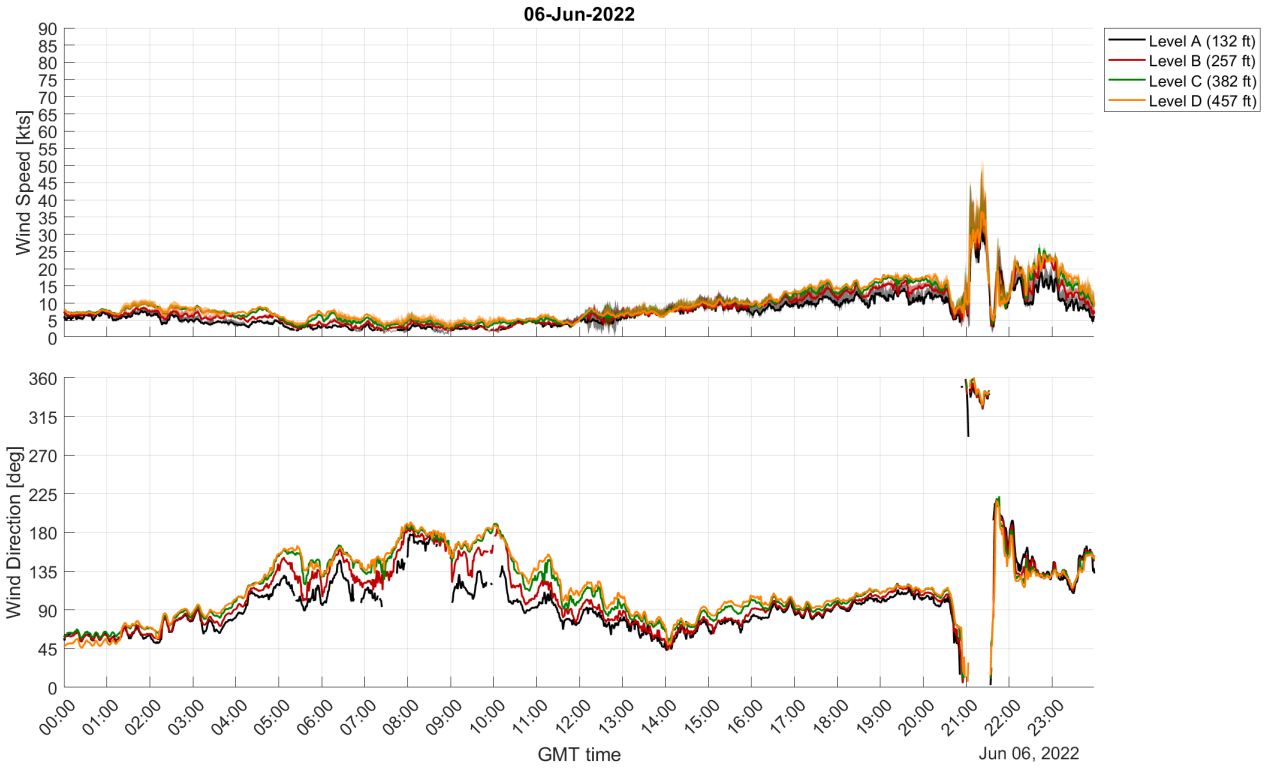

Fig. 27 Estimated wind speed and direction on the launch pad, June 6, 2022.

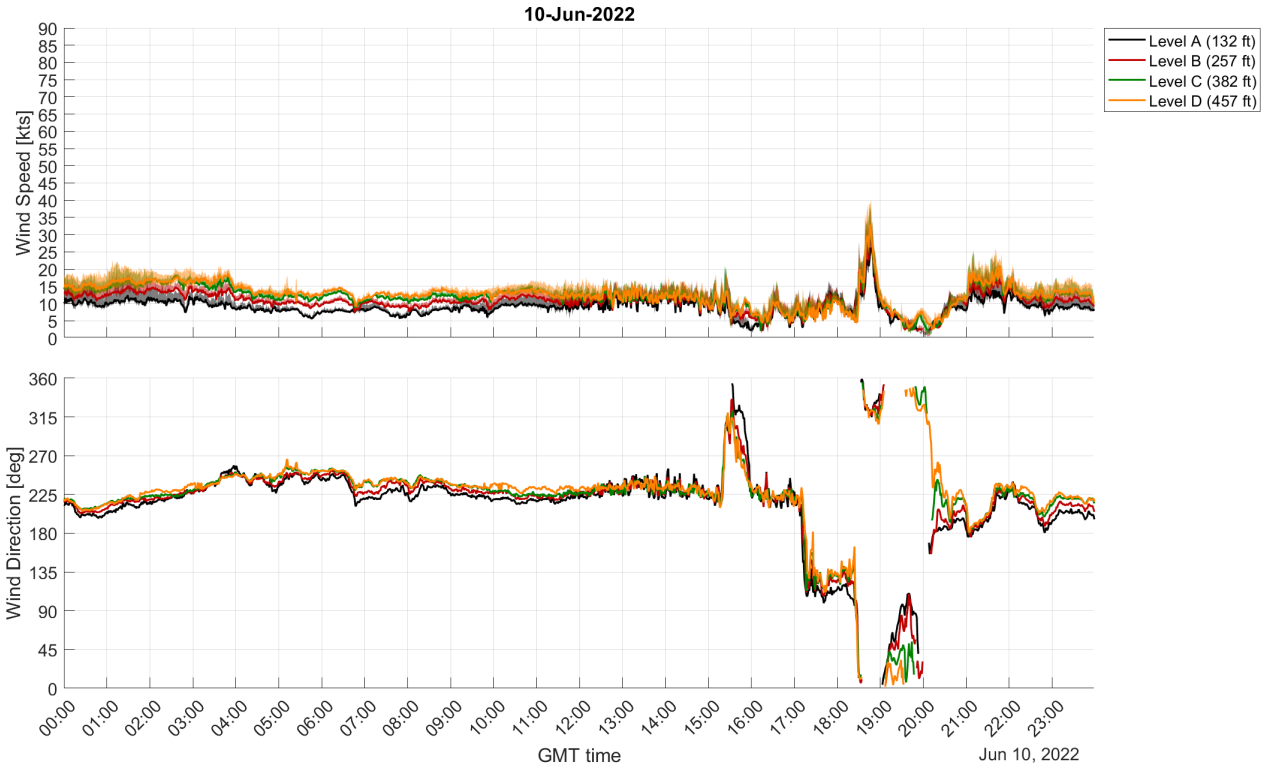

Fig. 28 Estimated wind speed and direction on the launch pad, June 10, 2022.

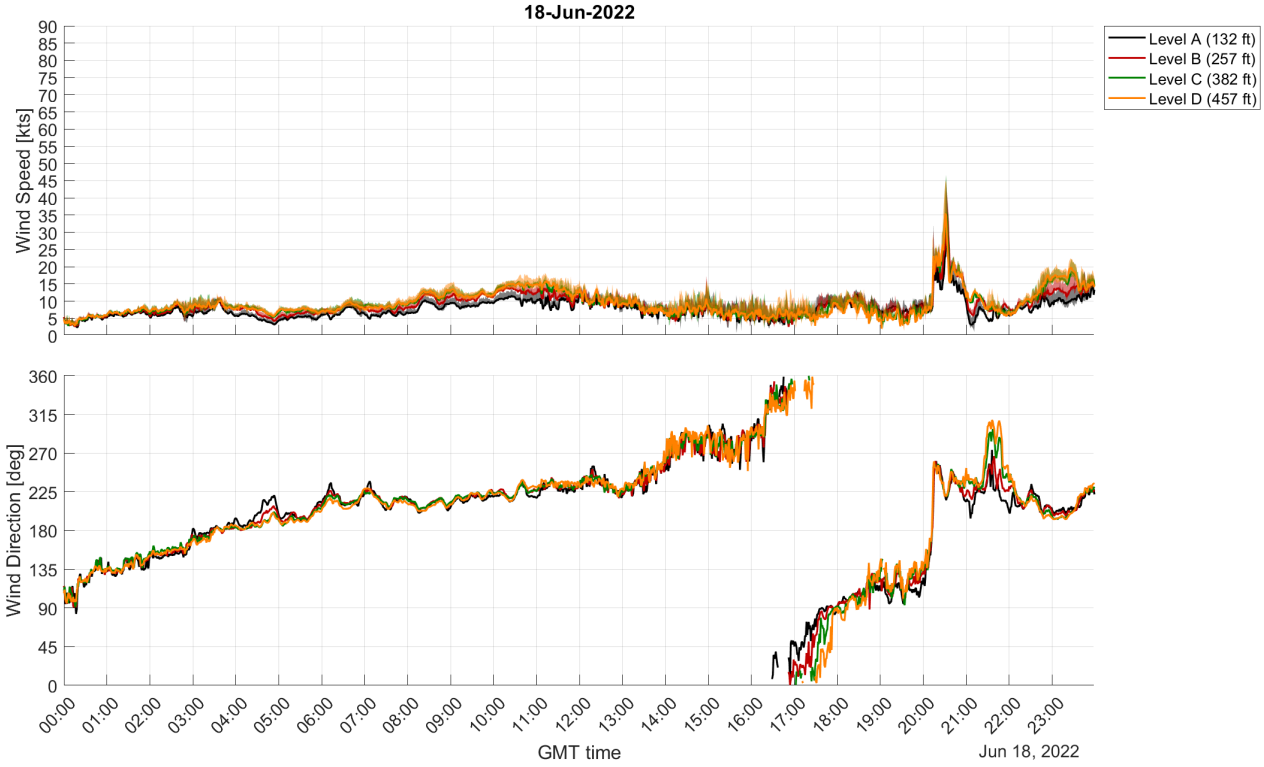

Fig. 29 Estimated wind speed and direction on the launch pad, June 18, 2022.

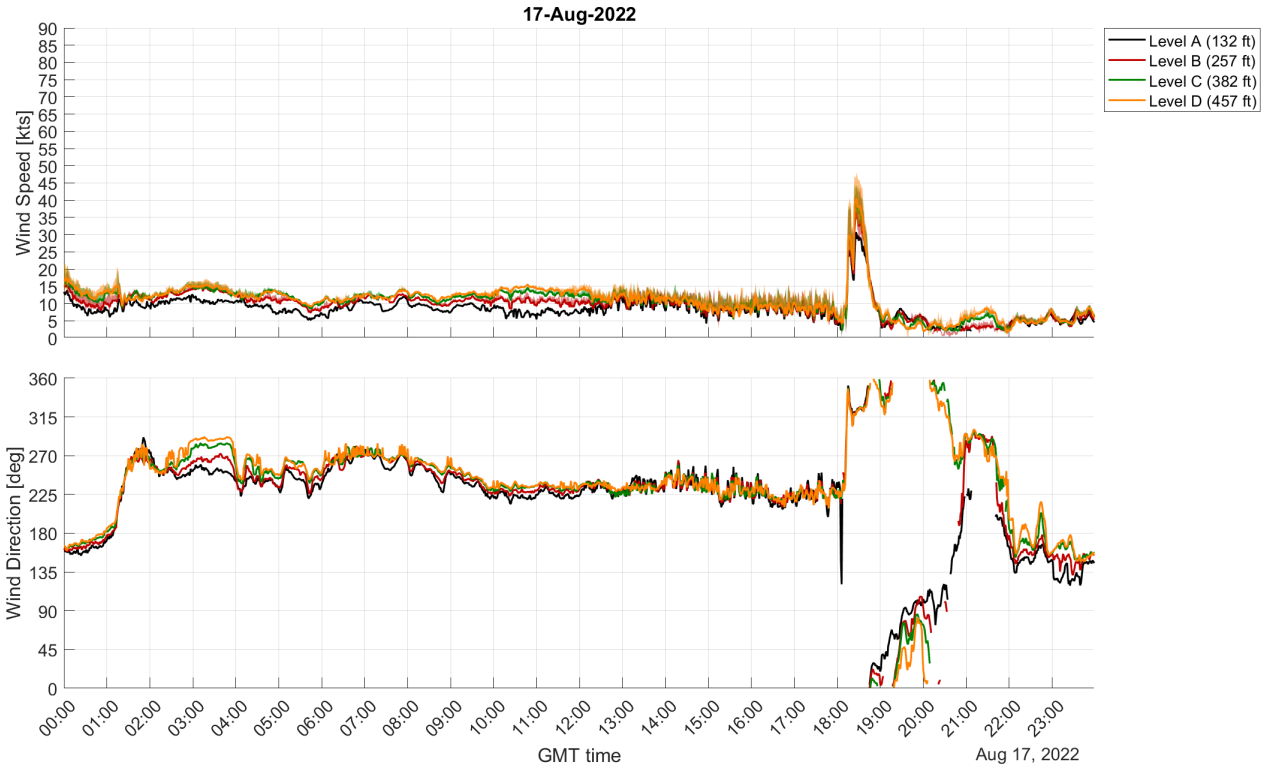

Fig. 30 Estimated wind speed and direction on the launch pad, August 17, 2022.

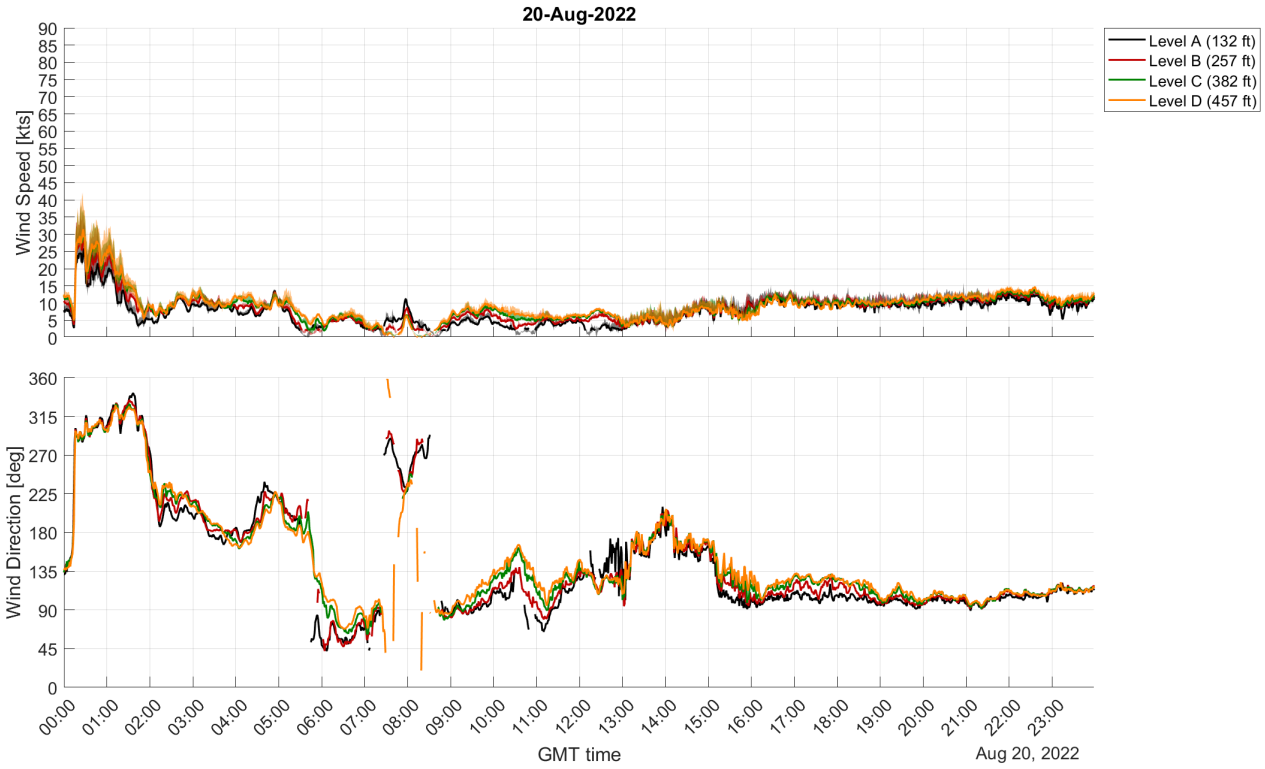

Fig. 31 Estimated wind speed and direction on the launch pad, August 20, 2022.

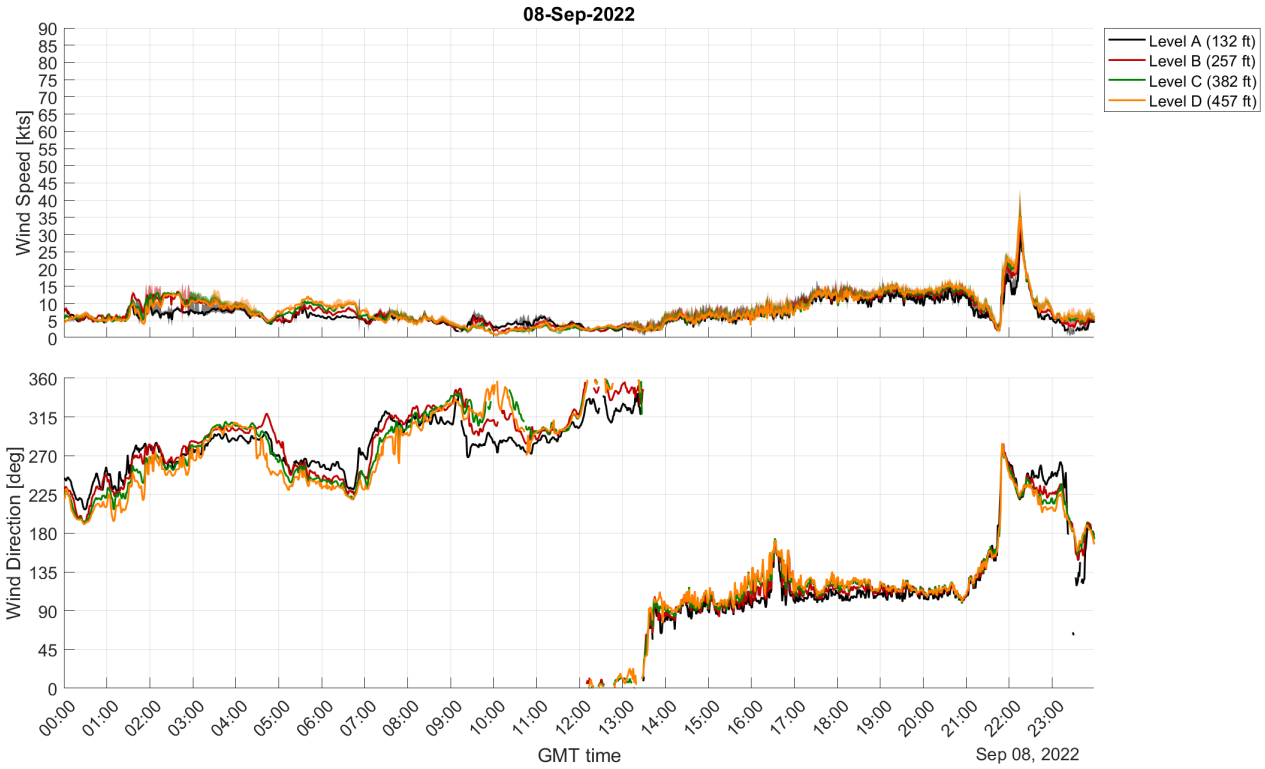

Fig. 32 Estimated wind speed and direction on the launch pad, September 8, 2022.

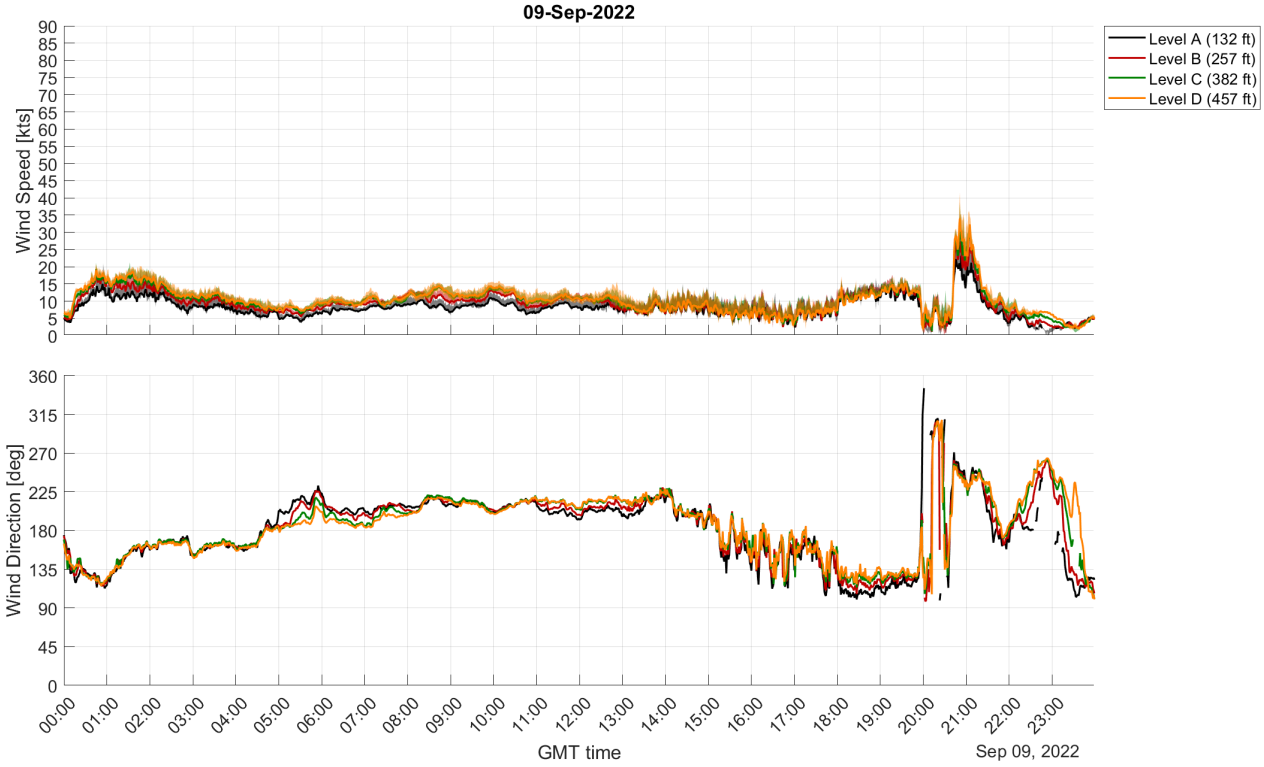

Fig. 33 Estimated wind speed and direction on the launch pad, September 9, 2022.

Fig. 34 Estimated wind speed and direction on the launch pad, September 10, 2022.

Fig. 35 Estimated wind speed and direction on the launch pad, September 12, 2022.

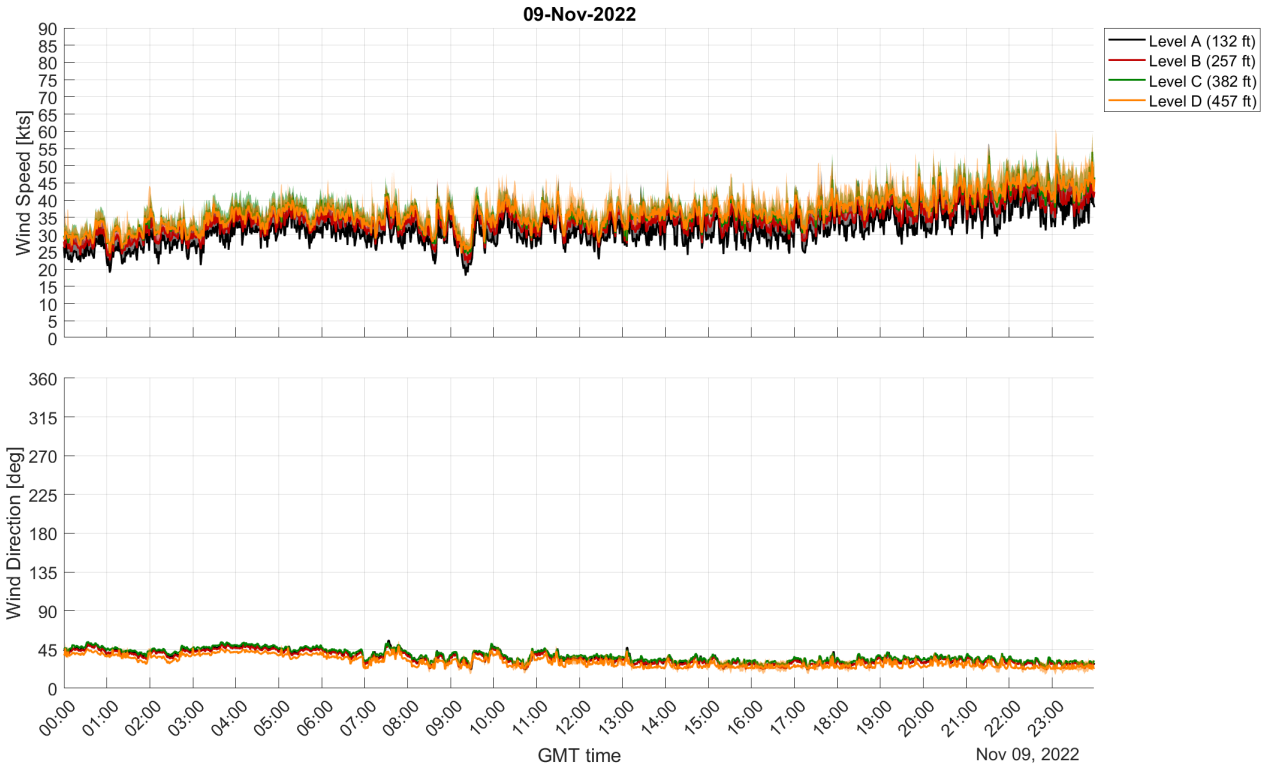

Fig. 36 Estimated wind speed and direction on the launch pad, November 9, 2022.

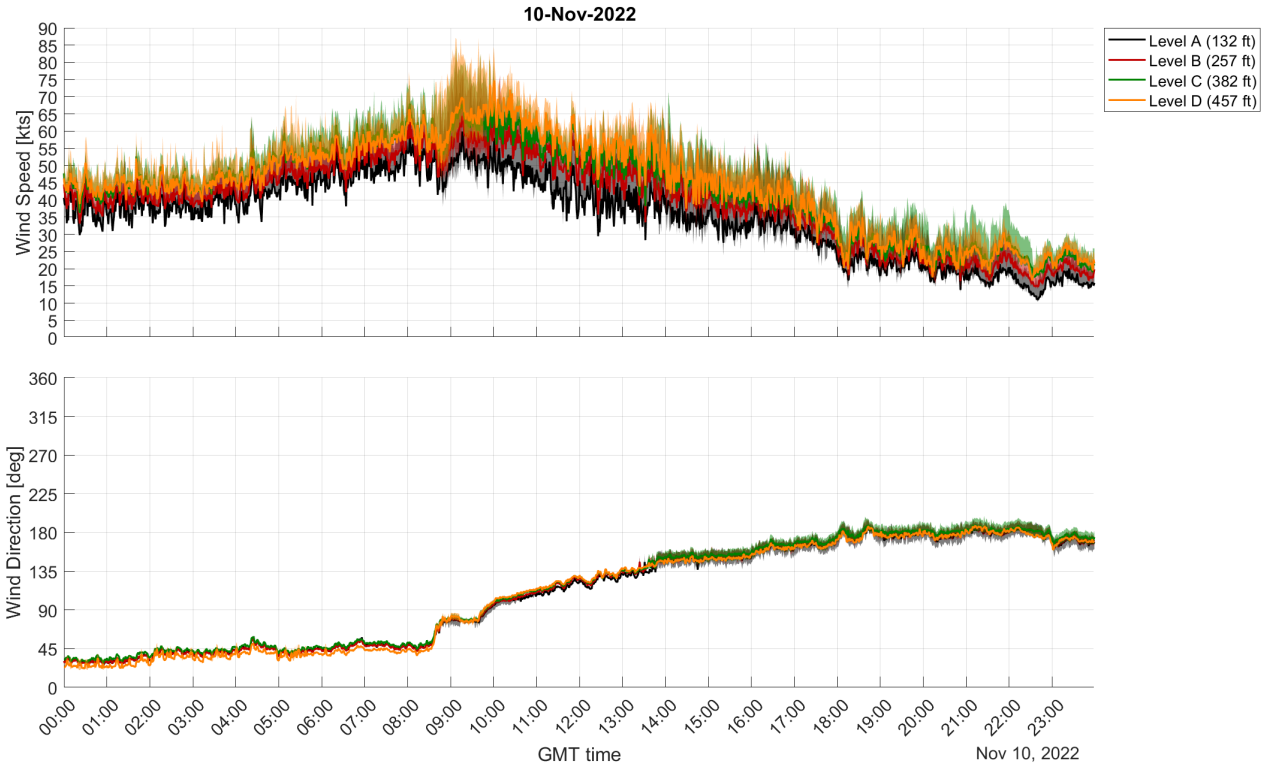

Fig. 37 Estimated wind speed and direction on the launch pad, November 10, 2022.

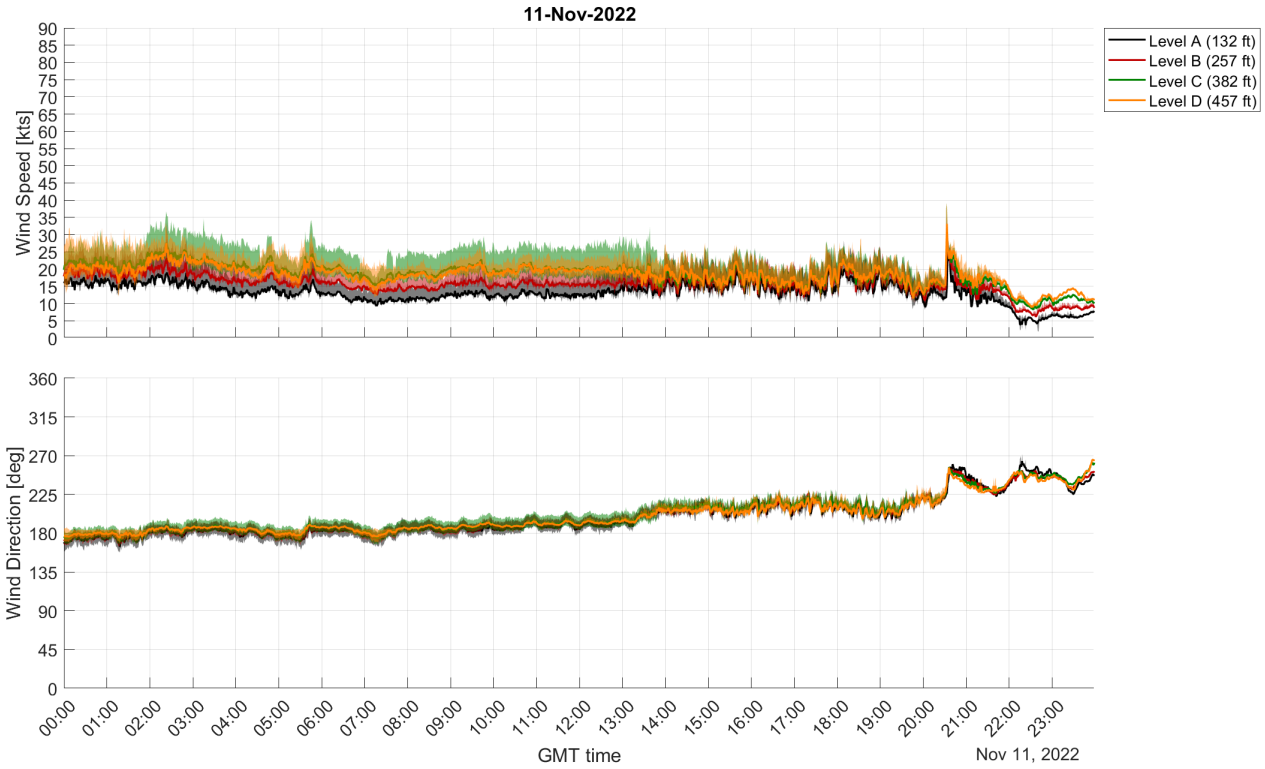

Fig. 38 Estimated wind speed and direction on the launch pad, November 11, 2022.

Acknowledgments

The author would like to acknowledge the support from the SLS Program Office at the NASA Marshall Space Flight Center and at the NASA Langley Research Center, as well as all SLS Aerodynamics Task Team members and leadership, past and present, from participating NASA Centers. The author would also like to thank the ground systems team (in particular Kevin Decker) for providing access to the ML sensor datasets, and the weather instrumentation group (in particular Tatiana Bonilla) for providing access to all prelaunch wind measurements from the LPS anemometers, both of these groups at the NASA Kennedy Space Center.

References

[1] "NASA's Space Launch System Reference Guide," Version 2, 2022.

[2] Blevins, J. A., Campbell, J. R., Bennett, D. W., Rausch, R., Gomez, R. J., and Kiris, C. C., "An Overview of the Characterization of the Space Launch System Aerodynamic Environments," *52nd AIAA Aerospace Sciences Meeting*, AIAA 2014-1253, 2014.

[3] Pinier, J. T., Herron, A. J., and Gomez, R. J., "Advances in the Characterization of NASA's Space Launch System Aerodynamic Environments," *2019 AIAA Aviation Forum*, AIAA 2019-3397, 2019.

[4] Pinier, J. T., Erickson, G. E., Paulson, J., Tomek, W. G., Bennett, D., and Blevins, J. A., "Space Launch System Liftoff and Transition Aerodynamic Characterization in the NASA Langley 14- by 22-Foot Subsonic Wind Tunnel," *53rd AIAA Aerospace Sciences Meeting*, American Institute of Aeronautics and Astronautics, AIAA 2015-0775, 2015. doi:doi:10.2514/6.2015-0775, URL http://dx.doi.org/10.2514/6.2015-0775.

[5] Chan, D. T., Paulson, J. W., Shea, P. R., Toro, K. G., Parker, P. A., and Commo, S. A., "Aerodynamic Characterization and Improved Testing Methods for the Space Launch System Liftoff and Transition Environment," *2019 AIAA Aviation Forum*, AIAA-2019-3398, 2019.

[6] Collins, J. G., Mears, L., Shea, P. R., Langston, S., Walker, M. A., and Pinier, J., "Improved Techniques for Measuring Static Ground Wind Loads on the NASA Space Launch System Mobile Launcher 2," *AIAA SCITECH 2023 Forum*, AIAA 2023-0424, 2023. doi:10.2514/6.2023-0424, URL https://arc.aiaa.org/doi/abs/10.2514/6.2023-0424.

[7] Mears, L., Shea, P. R., Collins, J. G., Langston, S., Walker, M. A., and Pinier, J., "Experimental Characterization of the Space Launch System Block 1B Liftoff and Transition Environment," *AIAA SCITECH 2023 Forum*, AIAA 2023-0423, 2023. doi:10.2514/6.2023-0423, URL https://arc.aiaa.org/doi/abs/10.2514/6.2023-0423.

[8] Wignall, T. J., Walker, M. A., and Collins, J. G., "Experimental and Computational Examination of the Coandă Effect on the Space Launch System at Liftoff Conditions," *AIAA SCITECH 2023 Forum*, AIAA 2023-0648, 2023. doi:10.2514/6.2023-0648, URL https://arc.aiaa.org/doi/abs/10.2514/6.2023-0648.

[9] Walker, M. A., Pinier, J. T., Shea, P. R., Collins, J. G., Mears, L., Lee, M. W., and Pomeroy, B. W., "Experimental Identification of Bistable Flow States on the Space Launch System at Liftoff Conditions," *AIAA AVIATION 2022 Forum*, American Institute of Aeronautics and Astronautics, AIAA 2022-3665, 2022. doi:doi:10.2514/6.2022-3665, URL https://doi.org/10.2514/6.2022-3665.

[10] Krist, S. E., Ratnayake, N. A., and Ghaffari, F., "Kestrel Results at Liftoff Conditions for a Space Launch System Configuration in Proximity to the Launch Tower," *2019 AIAA Aviation Forum*, AIAA 2019-3400, 2019.

[11] Ratnayake, N. A., Krist, S. E., and Ghaffari, F., "Selection of Computational Fluid Dynamics Tools Used in Development of the Space Launch System Liftoff and Transition Lineloads Databases," *2019 AIAA Aviation Forum*, AIAA 2019-3399, 2019.

[12] Pomeroy, B. W., "An Overview of NASA Langley Low-Speed CFD Contributions to the Space Launch System Program," *AIAA SCITECH 2023 Forum*, AIAA 2023-0236, 2023. doi:10.2514/6.2023-0236, URL https://arc.aiaa.org/doi/abs/10.2514/6.2023-0236.

[13] NASA, "SLS-SPEC-159: Cross-Program Design Specification for Natural Environments (DSNE)," Revision I, 2021.